NASA CR-175010

R85AEB304

National Aeronautics and
Space Administration

THERMAL BARRIER COATING LIFE PREDICTION MODEL

FIRST ANNUAL REPORT

By
R.V. Hillery
B.H. Pilsner

General Electric Company
Aircraft Engine Business Group
Cincinnati, Ohio 45215
April 1985

Prepared for
National Aeronautics and Space Administration

Lewis Research Center
Contract NAS3-23943

FORWARD

The First Annual Report, covering the period April 1984 to March 1985, was prepared by the Engineering Materials Technology Laboratories (EMTL) of General Electric's Aircraft Engine Business Group, Cincinnati, Ohio 45215, under NASA Contract NAS3-23943, R.V. Hillery of General Electric is the Principal Investigator and J.A. Nesbitt of NASA-LeRC is the Project Manager for NASA.

TABLE OF CONTENTS

LIST OF FIGURES

LIST OF TABLES

SUMMARY

This is the first annual report of the first phase of a 3-year program. The objectives are to determine the predominant modes of degradation of a plasma sprayed thermal barrier coating system, and then to develop and verify life prediction models accounting for these degradation modes. The first task (Task I) is to determine the major failure mechanisms. Presently, bond coat oxidation and bond coat creep are being evaluated as potential TBC failure mechanisms. The baseline TBC system consists of an air plasma sprayed ZrO_2-Y_2O_3 top coat, a low pressure plasma sprayed NiCrAlY bond coat, and a Rene' 80 substrate. Pre-exposures in air and argon combined with thermal cycle tests in air and argon are being utilized to evaluate bond coat oxidation as a failure mechanism. The first experiment has been completed. Unexpectedly, the specimens pre-exposed in argon failed before the specimens pre-exposed in air in subsequent thermal cycle testing in air. Investigations are underway to try to understand this result.

Four bond coats with different creep strengths are being utilized to evaluate the effect of bond coat creep on TBC degradation. These bond coats received an aluminide overcoat prior to application of the top coat to reduce the differences in bond coat oxidation behavior. Thermal cycle testing of these specimens has been initiated.

Preliminary experiments indicated that a Pt/Re layer at the bond coat/top coat interface was ineffective in retarding oxide scale growth, thus this proposed experiment covering this concept will be replaced by an experiment in which specimens are thermal cycle tested in argon.

Key property determination methods have been selected, and tensile strength, Poisson's ratio, dynamic modulus, and coefficient of thermal expansion will be determined.

INTRODUCTION

The objectives of this program are to determine the predominant modes of degradation of a plasma sprayed thermal barrier coating system, and then to develop and verify life prediction models accounting for these degradation modes. The program is divided into two phases, each consisting of several tasks. The Government will have the option to exercise Phase II after the first phase has been successfully completed.

The work in Phase I is aimed at identifying the relative importance of the various failure modes, and developing and verifying a life prediction model(s) for the predominant mode for a thermal barrier coating system. These objectives will be accomplished in a 36-month effort consisting of three technical tasks plus a reporting task. Task I will identify, through the design and performance of a series of experiments, the relative importance of the various failure modes for a base thermal barrier coating system. This TBC system consists of a low pressure plasma sprayed (LPPS) bond coat (0.13 $\pm$ 0.025 mm thick) and a plasma sprayed ZrO_2-8% Y_2O_3 top coat (0.25 $\pm$ 0.050 mm) on conventionally-cast Rene' 80 alloy substrate. Preliminary models will then be formulated based on analysis of the experimental data. These models will be tested and modified based on confirmation tests. Task I also includes determination of key properties of the coating materials such as tensile strength, Poisson's ratio, dynamic modulus, and coefficient of thermal expansion.

In Task II, life prediction models for the predominant failure modes will be developed. This will be accomplished by designing a suitable set of experiments and concomitant analyses, thus creating a life prediction model by means of a combined analytical, experimental program.

These models will be verified in Task III through a series of selected tests and analysis. The results obtained from this task should provide a better understanding of the life behavior of TBC systems and the suitability of the developed models. This understanding will be used to formulate recommendations for further research required to arrive at a fully satisfactory engine life prediction methodology.

The work in Phase II will develop design-capable, causal, life prediction models for thermomechanical and thermochemical failure modes, and for the exceptional conditions of foreign object damage and erosion. This will be accomplished in a 24-month effort consisting of five technical tasks plus a reporting task. In Task V, thermomechanical life models will be developed. This involves the development of models based on fracture and continuum mechanics, and possibly other life prediction models. In Task VI, thermochemical failure models will be developed, including oxidation and hot corrosion failure models. In Task VII, models for erosion and foreign object damage will be developed. The integration of appropriate combinations of models into a comprehensive life prediction model will be accomplished in Task VIII. In the final technical task, Task IX, the integrated model developed in Task VIII will be exercised through a combination of critical tests and analyses to determine its applicability and accuracy.

TASK I - FAILURE MECHANISM DETERMINATION

The objective of this task is to experimentally and analytically identify the relative importance of the various degradation and failure modes of the selected TBC system. Initially, a literature search was performed to assess current knowledge on potential failure mechanisms and how bond coat and top coat modifications affect these failure mechanisms. Spalling is currently considered the primary problem to be addressed for TBCs. As such, initial Task I efforts are directed at evaluating failure mechanisms associated with spallation.

Literature Search

Generally, state of the art thermal barrier coatings utilize two-layer coating systems. The systems consist of MCrAlX (M = Ni or Co or both; X=Hf, Zr, or Y) bond coats and ZrO_2-Y_2O_3 top coats. Three-layer systems have been investigated, (1,2) where an extra layer of "graded" bond coat and top coat material is incorporated between the bond coat and the top coat (to reduce the effect of thermal expansion mismatch). However, these three-layer systems have resulted in shorter thermal cycle life than two-layer systems (2). The shorter life is associated with significant oxidation of the bond coat material in the graded layer resulting from larger bond coat material surface area. Numerous studies have also shown that the composition and physical characteristics of both the bond coat and top coat are extremely important in determining thermal cycle life.

Bond Coating:

The primary role of the bond coat in a TBC system is to provide good adhesion between the metal substrate and the ceramic top coat, while providing good oxidation protection to the underlying substrate alloy. Numerous studies have demonstrated that oxidation of the bond coat can significantly affect spalling (3-6). For this reason, bond coat compositions have evolved from early Ni-Cr and Ni-Al compositions to the currently used MCrAlY compositions. Similarly, dense and more oxidation-resistant (lower levels of internal oxidation) bond coat layers produced by the low pressure plasma spray (LPPS) process have been shown to be better (longer thermal cycle life) than porous air plasma sprayed bond coat layers of the same chemical composition (1, 7). Both the chemical and processing changes have resulted in TBCs with longer thermal cycle lives.

Small changes in bond coat composition can also strongly affect thermal cycle life. Studies by Stecura have shown that the presence of small quantities of yttrium (0.1-1.0 wt.%) in the bond coat are critical (3). His studies indicate that TBC systems that utilize bond coats without yttrium fail very rapidly. Investigations have also shown that critical levels of Cr and Al are necessary to produce TBCs with long lives (3, 8). The same holds true for bond coat thickness, where a certain minimum thickness is required (3, 8). In all cases, changes to the bond coat have been linked primarily to improving the oxidation resistance of that layer.

Recent studies have been aimed at evaluating the effects of bond coat oxidation and developing models based on oxidation as a primary TBC failure

mechanism (9-11). In one study, Miller noted similar weight gains (oxidation) at failure of specimens with a $CaSiO_4$/MCrAlY TBC regardless of test temperature (9). Miller has also developed models based on thermal cycle and oxidation data (9, 11). His work has been primarily based on air plasma spray bond coats, but more recent work has shown that these models are applicable to LPPS bond coats (10). One model held on how oxidation affects failure is that oxidation strains are similar to thermal expansion mismatch strain (10). Thus, the strains of oxidation and the strains developed by thermal expansion mismatch are additive, and failure occurs once a certain level is reached.

There is recent General Electric evidence that by using stronger bond coat alloys, the thermal cycle life of TBC systems can be extended (12). TBCs with bond coat compositions of NiCrAlYZrB and NiCrAlYTaC (compositions based on NiCrAlY with additional grain boundary and solid-solution strengthening elements) had longer lives in thermal cycle testing than the conventional NiCrAlY bond coat. In another case, two bond coats with different creep strength were tested, and again, higher thermal cycle life was observed for the TBC system with the higher bond coat creep strength.

Bonding between the bond coat and ceramic layer of plasma-sprayed TBCs is largely mechanical, and the roughness of the bond coat is critical to keeping the ceramic layer attached (7). Therefore, the bond coat powder size and spray parameters must be adjusted to produce bond coat surfaces that have significant levels of surface roughness. However, care must be taken so that higher levels of porosity do not develop in the bond coat which would reduce oxidation resistance.

Top Coatings:

State of the art TBCs generally utilize ZrO_2 top coatings that have been partially stabilized with Y_2O_3 (13, 14). Recent investigations have shown that the optimum content is 6-8 w/o Y_2O_3 (15). Long thermal cycle lives have been obtained when these yttria-partially stabilized zirconia TBCs contain a large amount of the tetragonal phase, small but not zero (approximately 5%) monoclinic phase, and little or none of the cubic phase (16, 17). Stecura also noted that when no monoclinic zirconia phase was present and/or free yttrium was present in yttria stabilized zirconia containing 12% Y_2O_3 or more, the TBC fails rapidly (15). Unfortunately, little is known on how top coat phase changes actually affect thermal cycle life. Although, zirconia can be toughened by phase transformations (18, 19), it is doubtful plasma sprayed zirconia is toughened since a study in the grinding of the yttria-partially stabilized zirconia into a powder did not cause a significant amount of metastable tetragonal to transform to monoclinic (20). Also, fracture toughness was found to be rather insensitive to aging treatments (20).

The characteristics of the top coat powder can significantly affect thermal cycle life. In one study (21), nine different ZrO_2-8%Y_2O_3 top coat powders produced by various processes (spray-dried, sintered, etc.) were applied to TBC specimens and tested in a thermal cycle test under identical conditions. The thermal cycle life for these specimens ranged from 40-1000 cycles. These results demonstrate the importance of variations developed due to changes in top coat powder processing.

The levels of porosity and microcracks in the top coat can strongly affect thermal cycle life (22-24). Studies utilizing acoustic emission techniques have indicated that significant levels of microcracking, resulting from differences in thermal expansion mismatch, occur during the first few thermal cycles of testing of zirconia TBCs (25). It is believed that a ceramic coating that exhibits a high density of microcracking can better accommodate the differences in thermal expansion. Thus, the differences in thermal expansion are relieved by either the degree of plastic deformation or microcracking (26). Also, by decreasing top coat density, and thus hardness, the thermal shock resistance is enhanced with a concurrent increase in critical quench temperature *(23). In these cases, controlled porosity and microcrack levels (24) increase the toughness of the ceramic.

Bond Coat/Top Coat Interface

Generally, most authors have associated TBC failure with the development of compressive stresses that occur in the ceramic layer during cooling (5, 27). These stresses can be attributed to the thermal expansion mismatch between the ceramic top coat and metal bond coat (23, 26, 28, 29). However, these stresses may also be developed by plastic anistropy and thermal gradients introduced into the ceramic during plasma spraying (21). The importance of the stress has been shown by correlating TBC behavior to the substrate temperature during application of the top coat. By utilizing lower substrate temperatures, longer thermal cycle lives have been achieved (30, 31).

*In this study (23), the effect of zirconia coating density on thermal shock resistance was evaluated by rapidly quenching the coating into a water bath. The critical quench temperature was defined as the temperature required to cause coating failure or a large drop in coating hardness when quenched into the water bath.

Most TBC system failures appear to originate with the formation of a crack or cracks within the ceramic with failures occurring in the ceramic near the bond coat/top coat interface (17, 27). Analysis has indicated that, due to the development of temperature gradients in the ceramic, a state of biaxial compression and radial tension develops in the ceramic (5). This analysis also indicates that cooling stresses are more compressive at the bond coat/top coat interface and diminish toward the surface. Thus, failure can be attributed to the high stress state at this interface. As indicated, this higher stress state at this interface is primarily due to the thermal expansion mismatch which is probably effected by bond coat oxidation of the roughened bond coat surface.

Temperature and Thermal Cycle Duration

Higher temperatures and more rapid thermal cycling result in shorter TBC lives (5, 27). Stress calculations and experiments have indicated that repeatedly subjecting ceramic coatings to higher rates of initial heating and cooling has a more destructive influence on coating life than isothermal exposure at temperature (27). Higher substrate temperatures dramatically decrease thermal cycle life. This can be attributed to higher oxidation rates, larger ΔTs^* (which create larger stresses due to thermal expansion mismatch), and increased rates of other thermomechanical and thermochemical processes (such as interdiffusion, sintering, and corrosion).

* ΔT= maximum substrate temperature — minimum substrate temperature during a thermal cycle.

Other Potential Thermochemical Processes

Other potential thermochemical factors which can affect TBC life include sintering of the ceramic layer and interdiffusion between the bond coat and substrate. Because the plasma-sprayed zirconia layer consists of large particles (splats) and relatively large pores, shrinkage forces due to sintering are probably small. The more likely effect of sintering on TBC behavior is that which results from increased interparticle cohesion which, while increasing the strength of the ceramic layer (positive factor), may also reduce its strain tolerance (negative factor).

Interdiffusion of bond coat and substrate elements at elevated temperature does occur and has been documented (32) but the effect of such interdiffusion on TBC failure is not well defined. Clearly, the loss of aluminum from the bond coat by diffusion into the substrate can alter the oxidation behavior of the bond coat and in the extreme may lead to the formation of less adherent oxide species. Changing the composition of the bond coat layer and outer surface of the substrate through interdiffusion may also alter their physical and mechanical properties, and thus influence TBC behavior.

Corrosion of the bond coat, another thermochemical effect, can also lead to TBC failure. Corrosive attack of TBCs has not generally been a problem in aircraft engines, but can be a significant problem in marine and industrial applications. An additional mode of failure in corrosive environments is condensation of corrodant species in the pores of the ceramic layer, where it can do mechanical damage resulting from thermal expansion mismatch and/or volume changes associated with phase changes in the condensate. Corrosive

environments containing Na and V have also been observed to leach Y from yttria-stabilized zirconia leading to failure resulting from destabilization of the zirconia (33, 34). Reducing access of corrodants by partially sealing the surface of the zirconia coating by laser glazing has been shown to extend the life of TBCs in corrosive test environments (31), and the use of CeO_2 stabilized ZrO_2 has minimized destabilizations in V containing environments (32).

Other Failure Modes

Although spallation of the ceramic layer is the primary mode of TBC failure in current applications, erosion and impact damage are also important, potentially life-limiting causes for TBC degradation in engine environments. Loss of some of the ceramic layer by erosion has been observed in several engine test of TBCs, particularly on the outer bands of HPT nozzles. Plasma-sprayed ceramic layers of ZrO_2-Y_2O_3 have relatively low erosion resistance due to their unique structure and large amount (10% to 15%) of porosity, the same features that contribute to its ability to withstand thermal strain. It has been demonstrated that fusing the top few mils of the surface of the zirconia layer by a laser glasing process can increase the erosion resistance by a factor of 8 or more (31). Since only the outer few mils of coating are fused, the bulk of the zirconia layer retains the original strain tolerance.

Task I Efforts

One of the potential failure mechanisms being investigated in Task I is bond coat oxidation. As discussed above, many studies indicate that bond coat oxidation may be a major failure mechanism. Pre-exposures in air and argon were utilized to try to isolate the effect of bond coat oxidation on spalling.

Another failure mechanism being investigated is bond coat creep. As indicated, GE evidence has indicated that by using strong bond coat alloys, the thermal cycle life of TBC systems can be extended. In this part of the study, aluminide overcoats were applied to reduce the differences in bond coat oxidation between the various bond coats examined. It is believed that creep of the bond coat at elevated temperatures leads to a shift in the stress free temperatures and larger compressive stresses develop in the zirconia layer on return to room temperature, thus greater propensity for spalling.

Experimental Procedures

Specimen Preparation

The baseline system utilized consists of a low pressure plasma (LPPS) Ni-22Cr-10Al-0.3Y (wt. %) bond coat and an air plasma sprayed (APS) yttria-partially stabilized zirconia (ZrO_2-8%Y_2O_3) top coat on conventionally cast Rene' 80 alloy substrate (Table 1). Bond coat thickness was 0.13 $\pm$ 0.025 mm (0.005 $\pm$ 0.001 inch), and zirconia thickness was 0.25 $\pm$ 0.05 mm (0.010 $\pm$ 0.002 inch.)

The bond coat and top coat were applied to the tube specimen shown in Figure 1. The tube specimen was given the Rene' 80 solution heat treatment (1093°C (2000°F) for 2 hours, followed by 1093°C (2000°F) for 4 hours in vacuum) prior to application of the bond coat. The substrate surface was then grit blasted and vapor honed. The bond coat was applied on four specimens at a time using a planetary holder in an automated LPPS system. A bond coat powder size of -230+400 mesh was used to produce surface roughnesses greater than 400 μin in Ra*. (necessary to produce good bond coat/top coat bonding). Next, the bond coated specimens were cleaned in acetone and shadow masked. Shadow masking produced a tapered edge (Figure 2) on the zirconia coating layer to help reduce premature coating spallation during thermal cycle testing. The top coat was applied to each specimen individually using a GE P50 robot and a Metco Computerized Plasma Process Controller Spray System. The robot controls the plasma torch manipulations, while the Metco system controlled the spray parameters. The spray parameters used for both the bond coat and top coat are listed in Table II. The microstructure for this as-sprayed TBC system is shown in Figure 3.

*Ra is the average peak and valley height of the surface.

TABLE 1. BASELINE THERMAL BARRIER COATING SYSTEM (WEIGHT PERCENT)

Substrate (Rene'80): Ni-14Cr-9.5Co-5Ti-4W-4Mo-3Al-0.17C-0.03Zr-0.015B

Bond Coating : Ni-22Cr-10Al-0.3Y (Low Pressure Plasma Spray)

Top Coating : ZrO_2 - $8Y_2O_3$ (Air Plasma Spray)

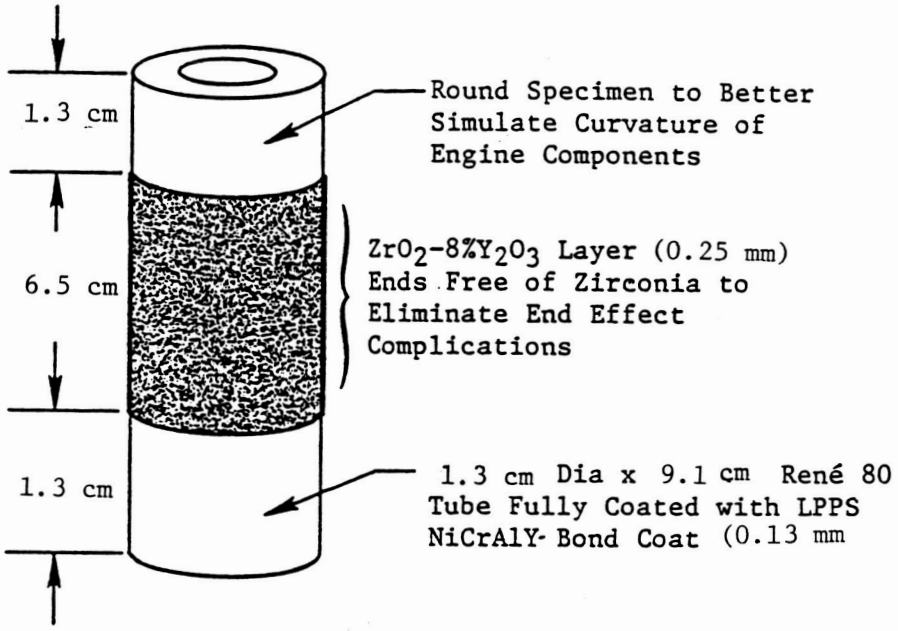

a) Test specimen configuration

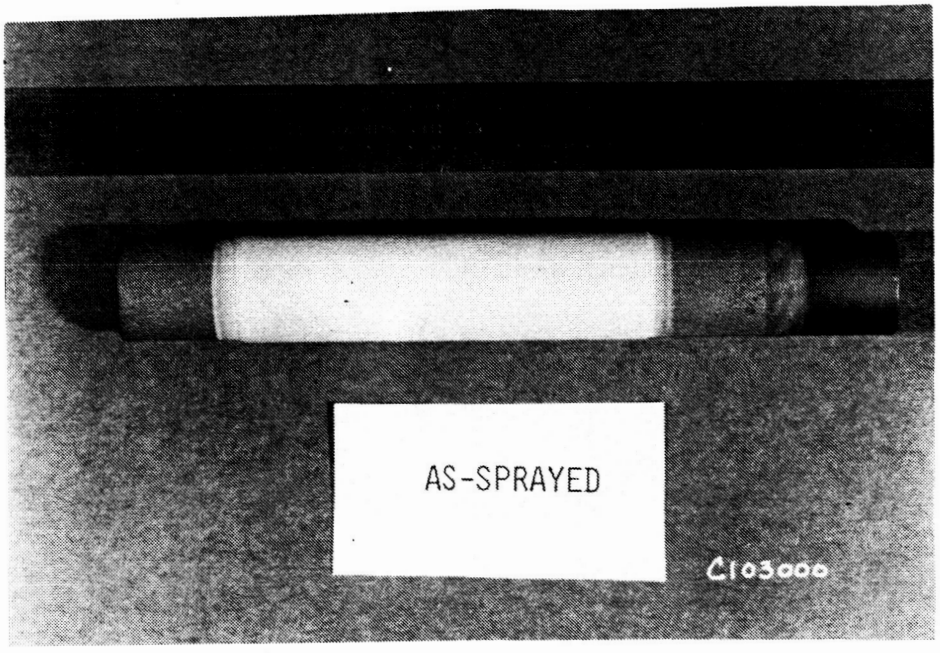

b) As-sprayed specimen

Figure 1 Thermal barrier coating test specimen

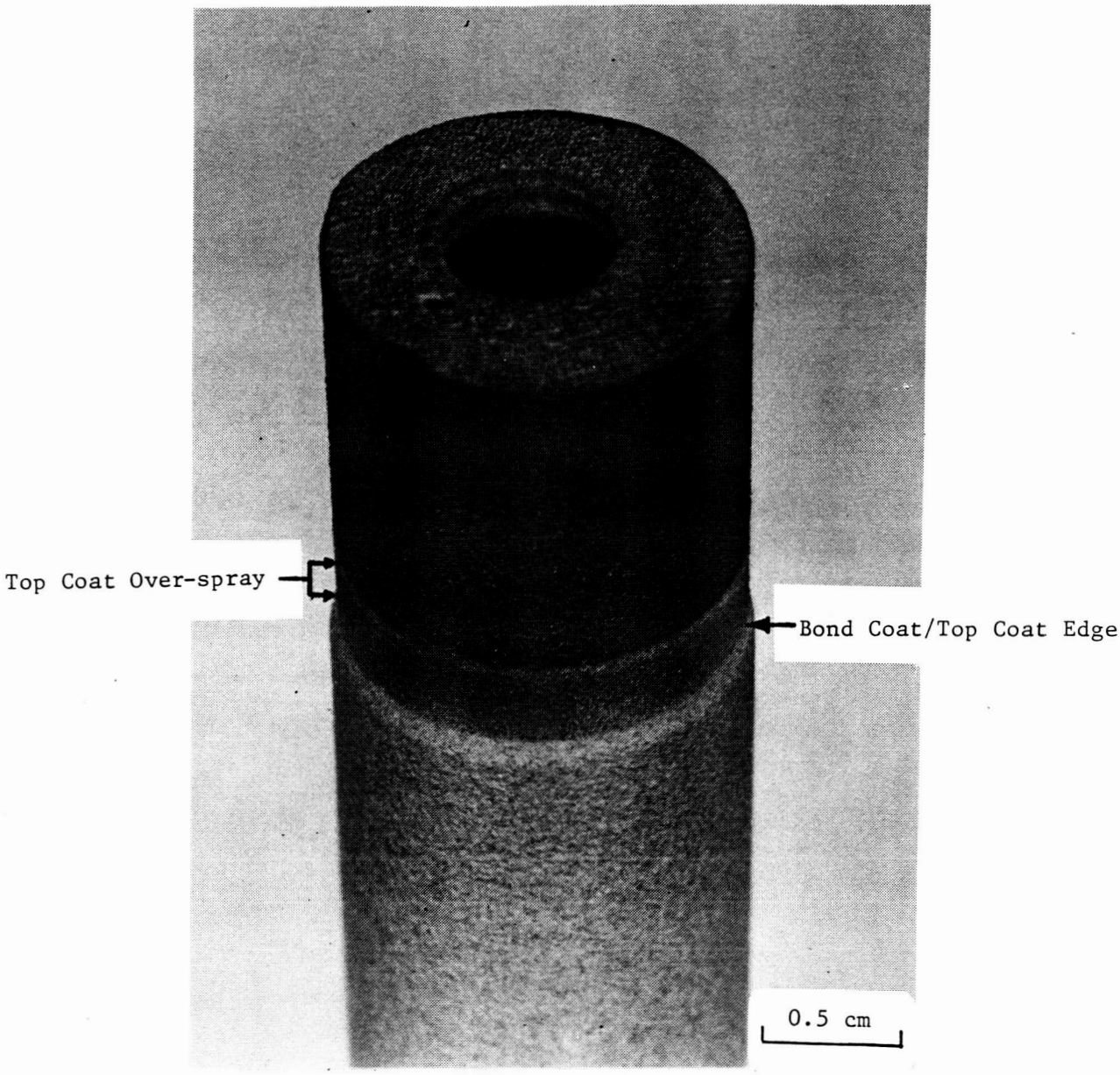

Figure 2 Tapered top coat edge developed by shadow masking

TABLE II

PLASMA SPRAY PARAMETERS

	APS	LPPS
Plasma Gun	Metco 7MB	Metco 7MB
Primary/Secondary Gas	N_2/H_2	Ar/H_2
Gun Power	36KW	50 KW
Powder Feed Rate	6 Lbs./Hr.	5 Lbs./Hr.
Preheat	-	1800°F
Spray Distance	5 In.	12 In.
Other	90° air impingement, and center of tube cooling.	Al_2O_3 grit blast and vaperhone cleaning.

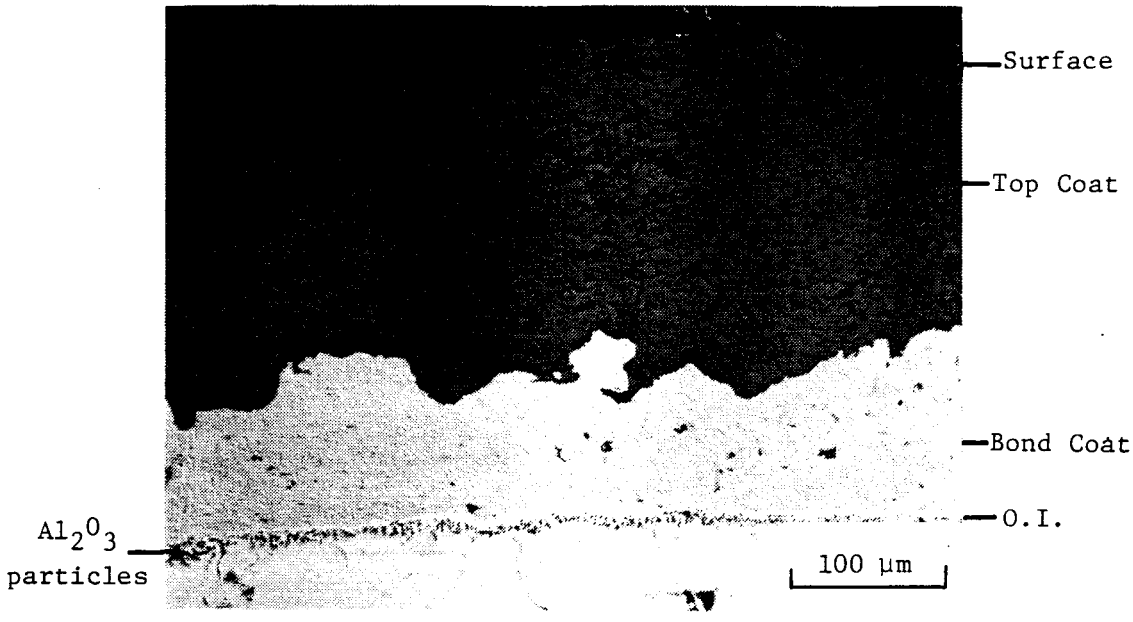

a) As-sprayed microstructure

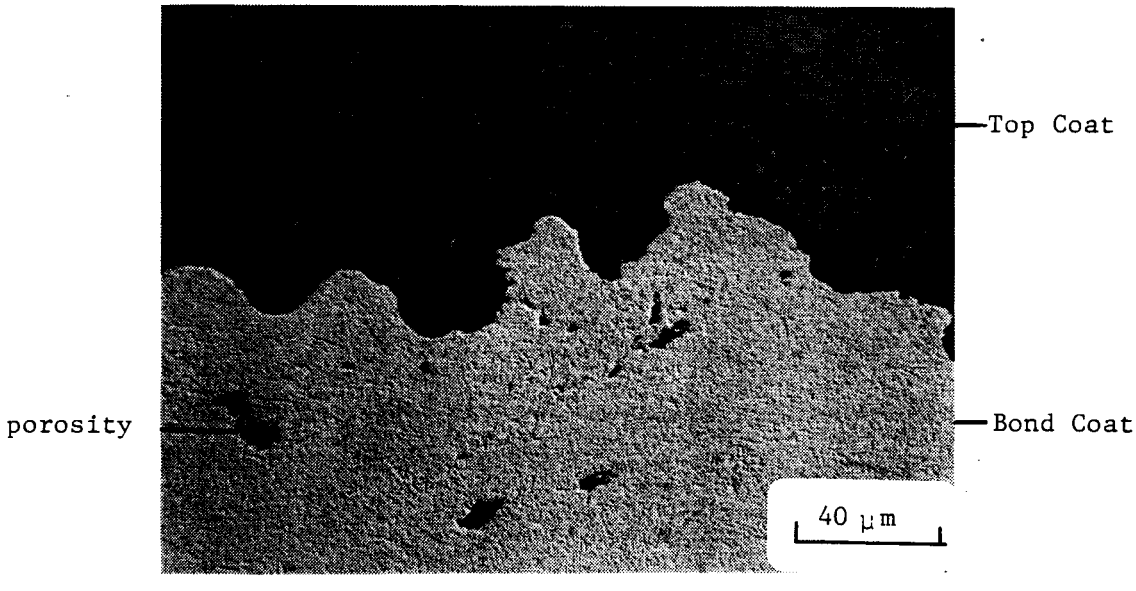

b) Bond coat/top coat interface

Figure 3 Baseline TBC as-sprayed microstructure (Rene '80, NiCrAlY, ZrO_2-Y_2O_3)

Bond Coat Oxidation Effect Experiments

Two experiments are being utilized to try to isolate the effects of bond coat oxidation on coating failure.

In the first experiment thermal cycle tests are being performed in air on specimens that have received isothermal pre-exposures in either static air or static argon. In this experiment, the thermal cycle lives of specimens that have been pre-exposed for selected times at 1093°C (2000°F) in inert (argon) and oxidizing (air) atmospheres are being compared. All pre-exposed specimens should contain "predamage" resulting from the thermally-activated processes other than oxidation, but only specimens pre-exposed in air should contain in addition the "predamage" due to oxidation (oxide scale growth on the bond coat). Thus, the difference in thermal cycle test lives of the two groups should reflect the effect of bond coat oxidation and allow evaluation of the magnitude of the other thermally-activated phenomena (sintering of the bond coat and zirconia layer, bond coat and ceramic coat creep, and bond coat/substrate interdiffusion).

Thermal cycling of the pre-exposed specimens was accomplished in a programmable, microprocessor controlled, rapid-heating furnace with $MoSi_2$ heating elements to a maximum temperature of 1093°C (2000°F) (Figure 4). The complete set of specimens (Table III) was cycled simultaneously. The thermal cycle was approximately 70 minutes long with approximately 10 minutes heat up, 45 minutes at temperature (1093°C), and 15 minutes forced air cooling. Specimens were removed from the test apparatus after every fifth cycle and visually examined for evidence of cracking and loss of the zirconia layer. Each specimen was removed from test when 10 percent of the zirconia layer had spalled. Selected specimens were evaluated metallographically.

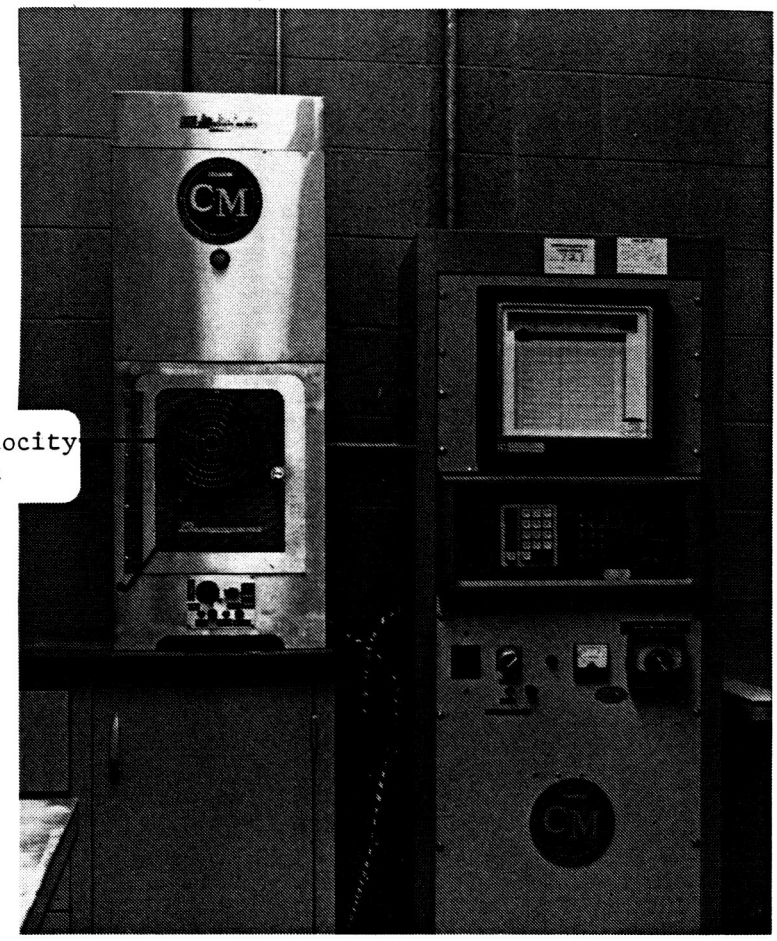

RAPID TEMPERATURE FURNACE

--- 10 minute heat up

--- 45 minute exposure at 2000 F

--- 15 minute forced air cooling

Figure 4 Rapid temperature thermal cycle furnace

TABLE III PRE-EXPOSURE (1093C) TIMES FOR BOND COAT OXIDATION EFFECT SPECIMENS (THERMAL CYCLE TESTING IN AIR)

Pre-Exposure Time (hours) at 2000 F.	Specimens Pre-exposed in Argon	Specimens Pre-exposed in Air
0	-	3
10	3	3
50	3	3
100	3	3
500	3	3
	12	15

TABLE IV PRE-EXPOSURE (1093C) TIMES FOR BOND COAT OXIDATION EFFECT SPECIMENS (THERMAL CYCLE TESTING IN ARGON)

Pre-Exposure Time (hours) at 2000 F.	Specimens Pre-exposed in Argon	Specimens Pre-exposed in Air
0	-	6*
100	3	6*
500	3	6*
	6	18

*Three specimens at each pre-exposure will be cycled in air to develop a baseline for these specimens contained in an Inconel 718 canister.

The second experiment is similar to the first except that the cyclic testing will be performed in static argon. This will be achieved by sealing specimens in argon filled Inconel 718 canisters (Figure 5) and thermal cycling them in the furnace described above. Argon pressure in the canisters will be adjusted to approximately 1 atmosphere at test temperature 1093°C (2000°F). Baseline specimens in unsealed canisters will also be included in the test to assess the effect of reduced heating and cooling rates. Five specimens will be sealed in the argon canister (five pre-exposure conditions) while three specimens will be cycled in the unsealed canister (three pre-exposure conditions). To provide triplicate testing, three sets of two canisters each will be cycled. To compensate for the slower cooling rate of specimens enclosed in canisters, the cooling period will be increased from 15 minutes to 30 minutes.

Specimens will be removed from the canisters at selected intervals for inspection. Fewer pre-exposures will be utilized than in the first experiment because of the added experimental difficulties. Planned pre-exposure times are listed in Table IV, but may be modified based on experimental results from the first experiment (described above). Specimens for this experiment have been coated with TBC and await pre-exposure.

Pt/Re Experiments

It was originally planned to include specimens in the thermal cycle tests that had thin layers of Pt and Re between the bond coat and the zirconia layer. The intent was that the Re layer would reduce the access of oxygen to the bond coat and thus reduce the formation of oxide scale on it. The intended purpose of the Pt layer between the top coat and the Re layer was to reduce the volatile interaction between the Re and oxygen.

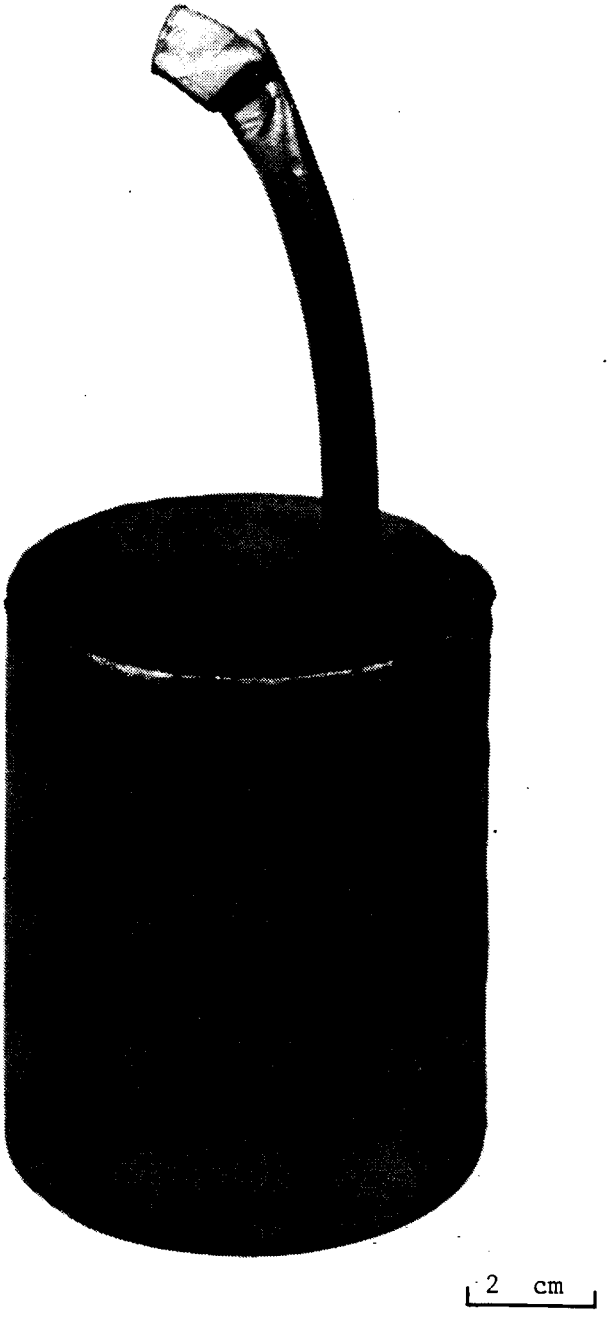

Figure 5 Inconel 718 canister utilized for thermal cycle testing in argon

Preliminary tests, however, showed these Pt/Re layers to be ineffective in significantly retarding oxide scale formation. Specimens with the Pt/Re layers were exposed in static air at 1093° (2000°F) for 168 hours along with baseline specimens (no barrier layer). Microstructural examination revealed that a continuous oxide scale was present on specimens with the Pt/Re layers as well as on the baseline specimens. The primary difference was that the oxide scale formed at the plating/top coat interface in the Pt/Re specimens, whereas it formed at the usual location (bond coat /top coat interface) in the baseline specimens. The presence of the Pt/Re layer resulted in only small decreases in oxide scale thickness (3 μ m versus 4 μ m). This may be attributable to the time necessary for Al from the bond coat to move through the plating to the plating/top coat interface.

Based on these results, the use of Pt/Re layers to retard oxide scale growth was discontinued, and instead an experiment was designed in which thermal barrier coated specimens will be thermal cycled in an inert (argon) environment (as described earlier).

Bond Coat Creep Effect Experiment

The experiment to evaluate the effect of bond coat creep strength on thermal cycle life utilized four different bond coat alloys (Table V) that have significantly different creep strengths. The modified NiCrAlY bond coats include additions of Co, Mo, Ta, W, Re, Hf, C, B, Si, Zr, and Ti. The bond coat layers on these specimens also received a Codep (aluminide) coating (Figure 6) before the ceramic layer was deposited to reduce the effect of any differences in oxidation resistance on thermal cycle life. All specimens were coated with the same ZrO_2-8%Y_2O_3 ceramic layer. Nine specimens of each

Table V BOND COAT CREEP EFFECT TBC SYSTEMS

Systems	Substrate / Bond Coating / Over Coating/ Top Coating	Bond Coat Creep (Larson/Miller Parameter @ 3 KSI - rupture test)
1	Rene'80 / Bond Coating 1' / Aluminide / ZrO_2-Y_2O_3	39.0
2	Rene'80 / Bond Coating 2* / Aluminide / ZrO_2-Y_2O_3	45.7
3	Rene'80 / Bond Coating 3* / Aluminide / ZrO_2-Y_2O_3	47.0
4	Rene'80 / Bond Coating 4* / Aluminide / ZrO_2-Y_2O_3	48.4

' Ni-22Cr-10Al-0.3Y

* Modified NiCrAlY bond coats

TABLE VI PRE-EXPOSURE (1093C) TIMES FOR BOND COAT CPREEP EFFECT SPECIMEN (THERMAL CYCLE TESTING IN AIR)

Alloys	Specimens With No Pre-exposure	Specimens Pre-exposed in Argon (2000F, 100 hrs)	Specimens Pre-exposed in Air (2000F, 100 hrs)
1	3	3	3
2	3	3	3
3	3	3	3
4	3	3	3
	12	12	12

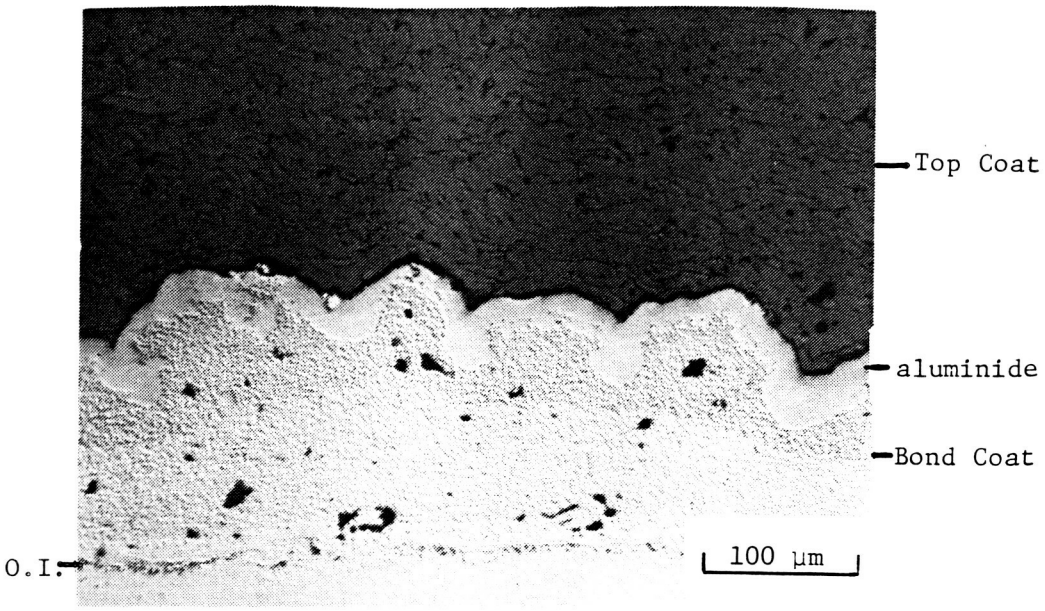

a) As-sprayed microstructure

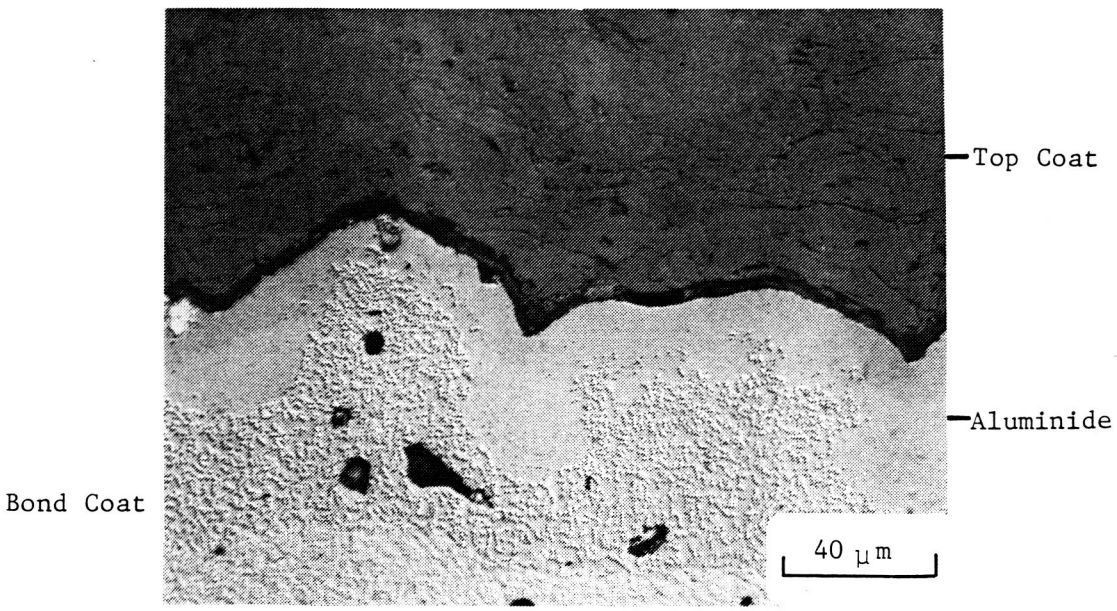

b) Bond coat/top coat interface

Figure 6 Microstructure of as-sprayed TBC with aluminide coated bond coat(Rene '80/NiCrAlY/Aluminide/ ZrO_2-Y_2O_3)

TBC have been prepared for thermal cycle testing. Three specimens were exposed in argon for 100 hours at 1093°C (2000°F), three were exposed in air for the same time and temperature; three specimens received no pre-exposure (Table VI). The difference in thermal cycle lives should be a function of bond coat creep strength and pretest conditions. The intent of this experiment is to evaluate the effect of bond coat creep strength on TBC failure and to obtain a measure of its effect relative to that of oxidation.

RESULTS

Pre-Exposures

Surface Appearance

The surface appearances of the specimens pre-exposed in the two different environments (argon and air) were indicative of those environments. The argon atmosphere exposures at 1093°C (2000°F) produced clean unoxidized bond coat surfaces, while the ceramic top coat had a gray appearance which can be attributed to oxygen deficiency (Figure 7a). This gray appearance is common for TBCs that receive vacuum or inert atmosphere heat treatments. The air atmosphere exposure at 1093°C (2000°F) produced oxidized bond coat surfaces, while the ceramic top coat had a straw colored, appearance typical of elevated temperature air exposure (Figure 7b).

Microstructure

In all cases, a continuous Al_2O_3 scale formed at the bond coat/top coat interface in specimens that were pre-exposed in air at 1093°C (2000°F). The oxide scale thickness varied from 2 μm to 6 μm for the different pre-exposure times (Figure 8) for the baseline TBC system. The oxide scale thickness varied from 3 μm - 5μ m for the four different bond coat systems that were pre-exposed in air for 100 hours (bond coat creep effect specimens)(Table VII). The formation of the Al_2O_3 scale resulted in β depletion (high Al phase, NiAl type structure) in the bond coat at the bond coat/top coat interface (Figures 9&10)*. Depletion of the high Al β phase also occurred in the bond coat at the bond coat/substrate interface due to interdiffusion. This interdiffusion also resulted in formation of high Cr particles (presumably $M_{23}C_6$ carbides) in both the bond coat and

* Etchant: 10% phosphoric acid, 90% water (3-5 volts applied)

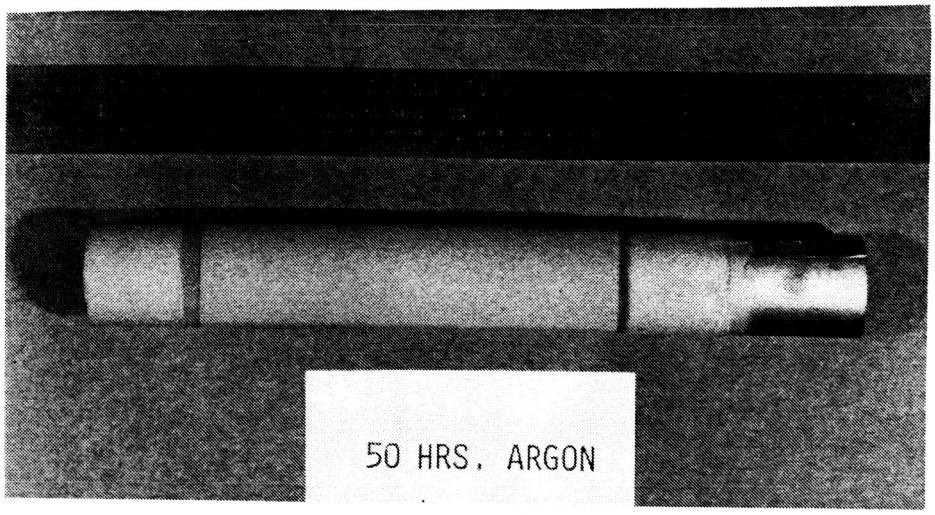

a) 50 hour argon pre-exposure

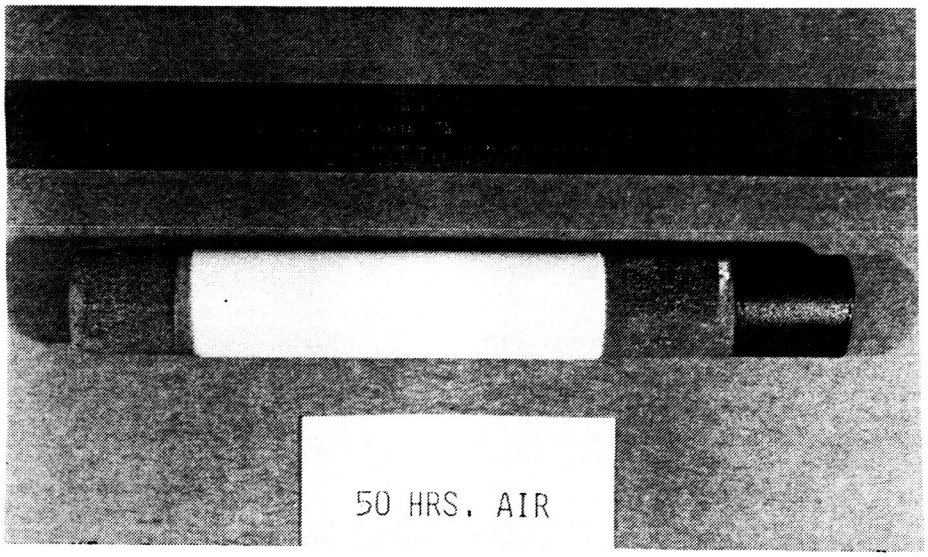

b) 50 hour air pre-exposure

Figure 7 TBC specimens after receiving air or argon pre-exposures at 1093C(2000F)

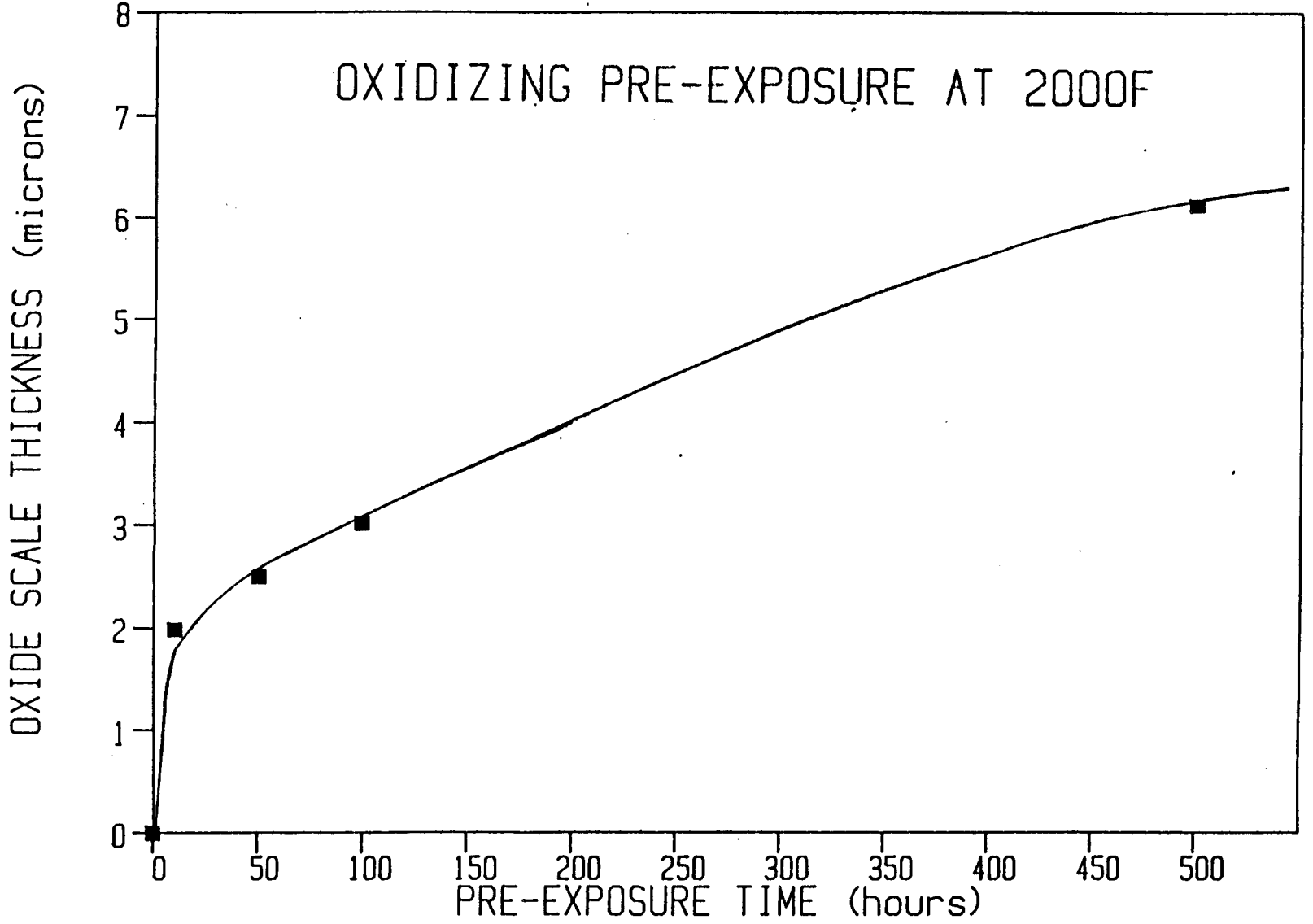

Figure 8 Oxide scale thickness at bond coat/top coat interface after air pre-exposures at 1093C(2000F)

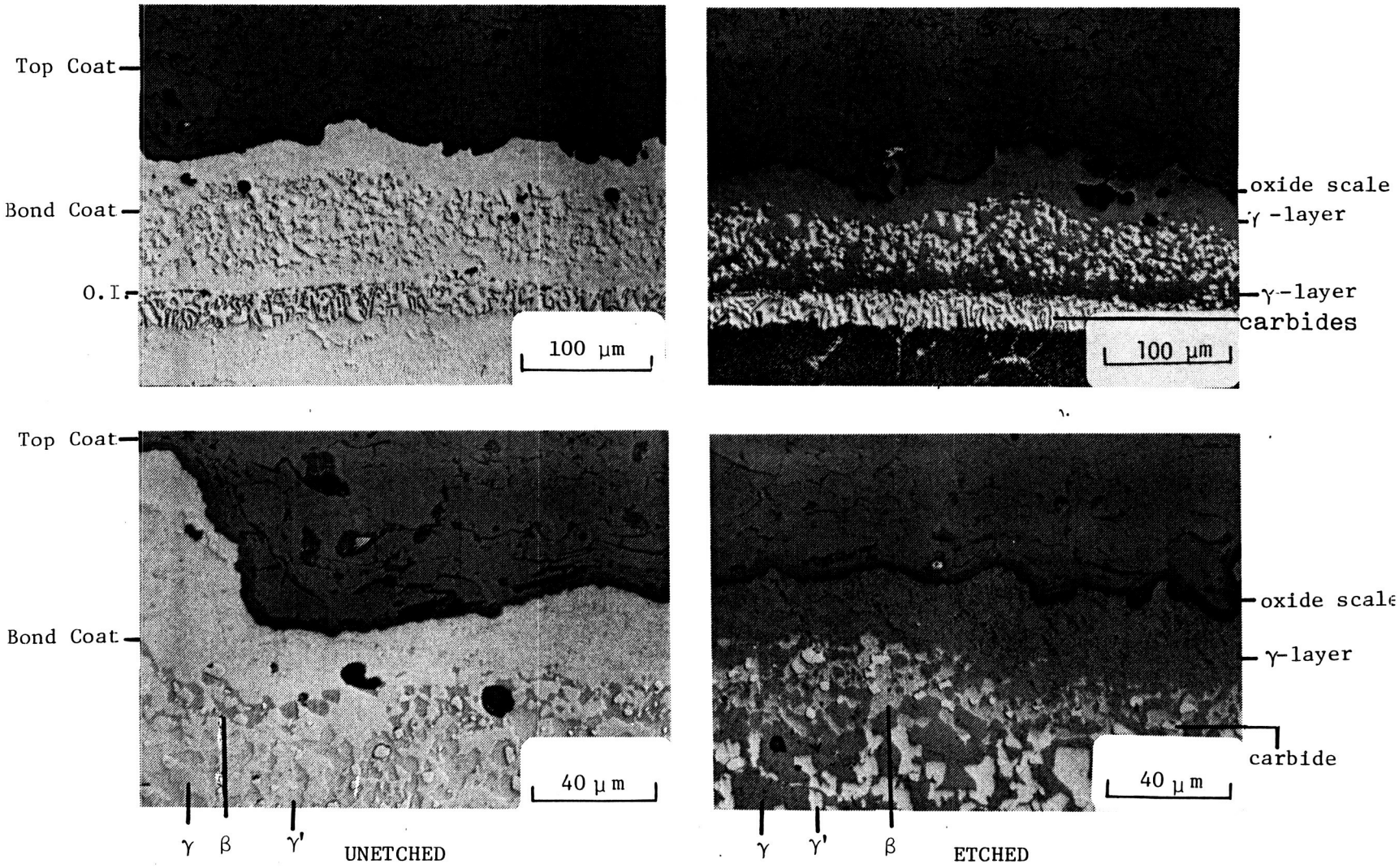

Figure 9 Microstructure after 100 hour air pre-exposure at 1093C(2000F)

TABLE VII OXIDE SCALE THICKNESS AT BOND COAT/TOP COAT INTERFACE AFTER 100 HOUR AIR PRE-EXPOSURE (1093C) FOR THE BOND COAT CREEP EFFECT SPECIMENS

BOND COATING	OXIDE SCALE THICKNESS (μm)
1	3.0
2	5.3
3	2.8
4	4.3

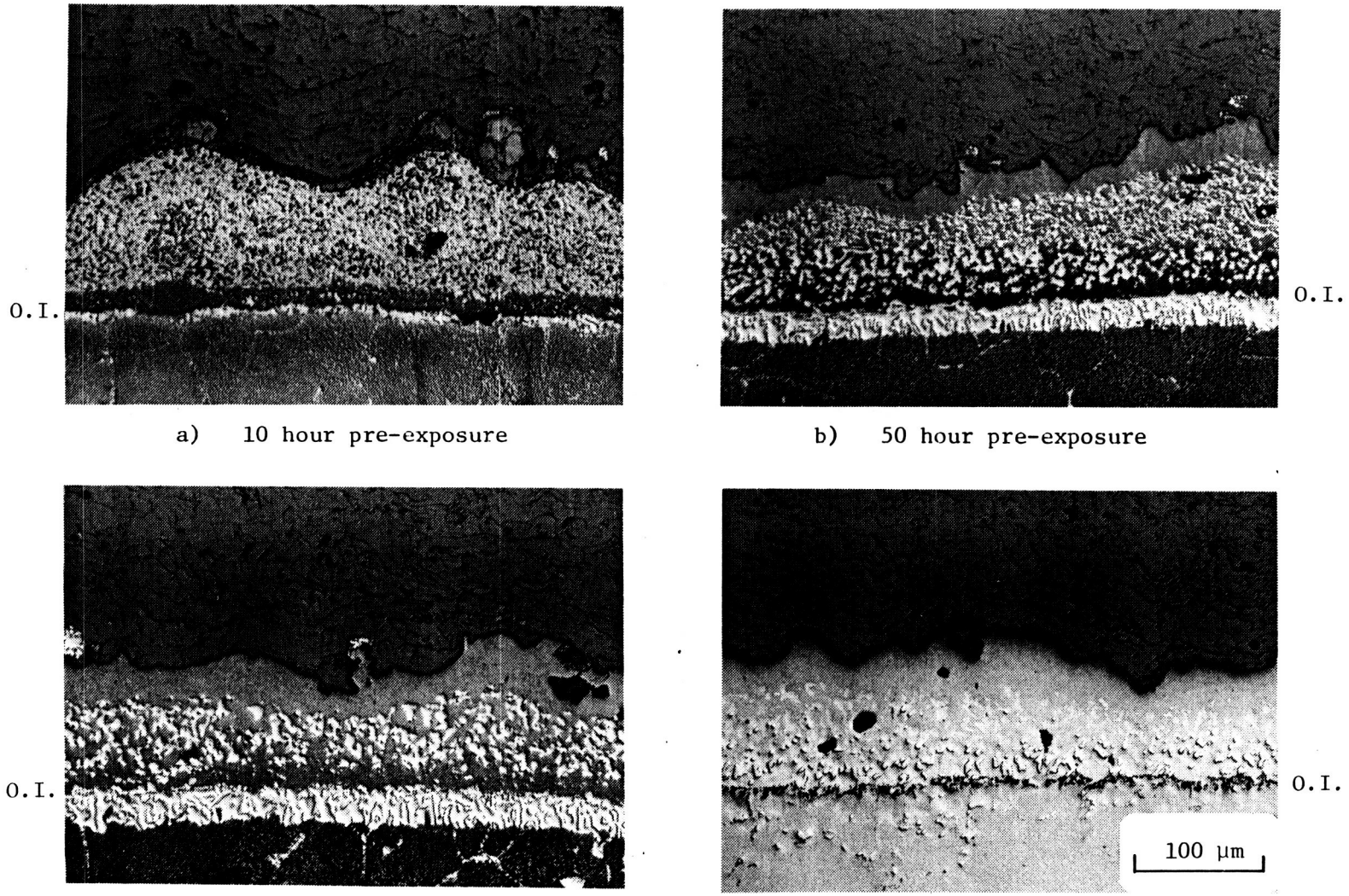

a) 10 hour pre-exposure

b) 50 hour pre-exposure

c) 100 hour pre-exposure

d) 472 hour pre-exposure

ETCHED

Figure 10 Microstructures of specimens pre-exposed in air at 1093C(2000F)

substrate near this interface. These carbides generally are not harmful since failure does not normally occur in these TBC systems at the bond coat/substrate interface. It was observed that in all cases the Al_2O_3 scale is highly adherent to both the bond coat and the top coat.

The use of canisters containing argon was very effective in retarding oxidation during pre-exposure at 1093°C (2000°F)*. In all cases except one, essentially no Al_2O_3 was detected at the bond coat/top coat interface by optical microscopy after pre-exposure (Figures 11,12). The exception was the 472 hour pre-exposure where a leak developed in the argon canister system at approximately that point in time. Both the air and argon pre-exposures were terminated at this point instead of the 500 hour planned exposure. Therefore, the specimens referred to as being pre-exposed for 500 hours were actually pre-exposed for 472 hours. The argon leak resulted in the development of traces of Al_2O_3 scale at the bond coat/top coat interface for these specimens (Figure 12). The growth of these traces did result in some β depletion at the top coat/bond coat interface, whereas all other argon pre-exposure specimens had negligible β depletion at this interface. The formation of $M_{23}C_6$ carbides and β depletion in the bond coat can again be seen at the bond coat/substrate interface. The bond coat/top coat interface (Figures 11,12) of the argon pre-exposed specimens did not appear to have the high degree of adherence that the air pre-exposure specimens which had formed a continuous Al_2O_3 scale (Figures 9,10 vs. Figures 11,12).

* The change in weight was measured after both the 100 hour argon and 100 hour air pre-exposures for the bond coat creep effect specimens. The air pre-exposures exhibited 0.62-0.90 mg/cm^2 weight gains, while the argon pre-exposures exhibited 0.07-0.35 mg/cm^2 weight losses.

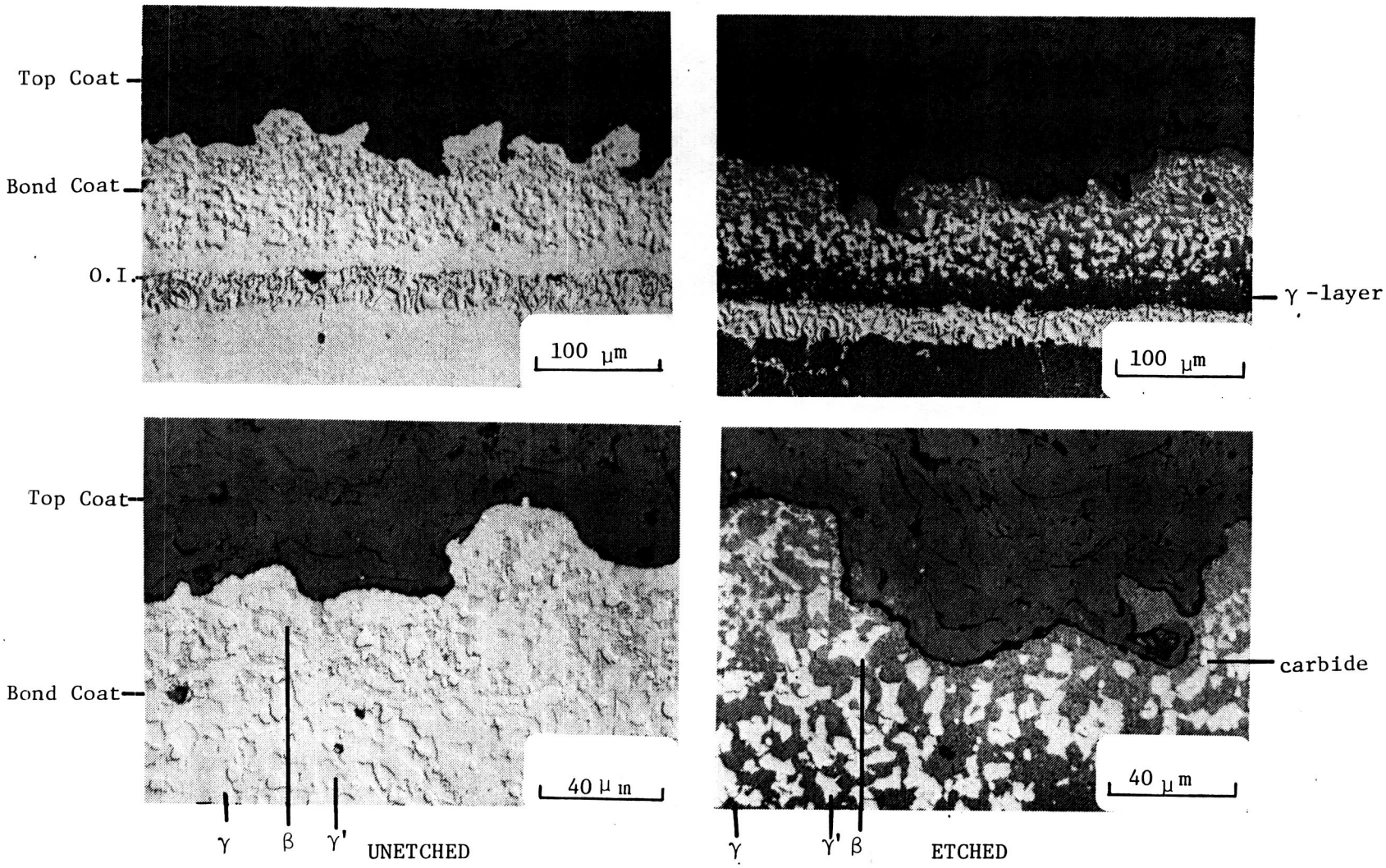

Figure 11 Microstructure after 100 hour argon pre-exposure at 1093C(2000F)

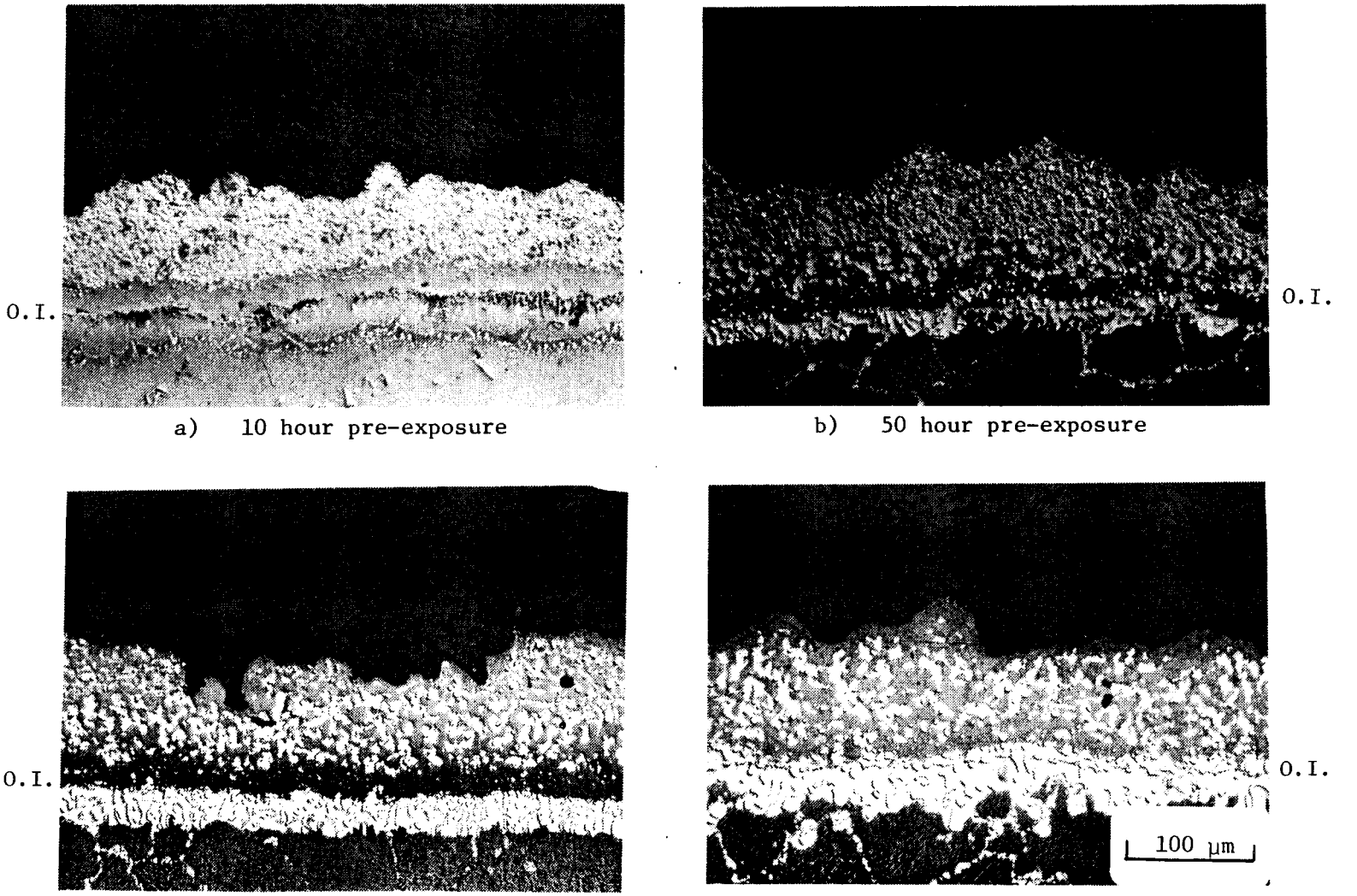

a) 10 hour pre-exposure

b) 50 hour pre-exposure

c) 100 hour pre-exposure ETCHED

d) 472 hour pre-exposure

Figure 12 Microstructures of specimens pre-exposed in argon at 1093C(2000F)

Concentration/Distance Profiles

Concentration/distance profiles (Electron Microprobe) were determined for the baseline specimens at each of the pre-exposure conditions. The profiles assess the compositional changes that the bond coat experienced during the pre-exposure via interdiffusion and oxidation. Probe measurements were taken in the top coat, bond coat, and substrate. However, the measurements indicated that very little interdiffusion occurred between the top coat and bond coat. Based on these findings, the concentration/distance profiles shown include only bond coat and substrate measurements (Figures 13,14,15,&16). The profiles should be considered semi-quantitative since a two or three phase structure is still present in the bond coat and in the substrate after pre-exposure. The scatter observed in the profiles can be attributed to analysis from this 2 or 3 phase structure.

The profiles for Al (Figure 14a,b,c,&d) show the increasing loss of Al from the bond coat to form Al_2O_3 scale at the bond coat/top coat interface and into the substrate via interdiffusion caused by increasing pre-exposure time. In all cases, a lower Al level is present at the bond coat/top coat interface for the specimens pre-exposed in air. However, the Al profiles also indicate that bond coat/substrate interdiffusion is more significant in reducing the quantity of Al present in the bond coat.

Significant interdiffusion has occurred for the other elements such as Cr, W, Ti, Co, and Mo (Figures 14,15,&16). Significant quantities of Cr have moved from the bond coat into the substrate, while significant quantities of Ti, Co, W, and Mo have moved into the bond coat from the substrate. These transferred quantities also increased substantially with pre-exposure time.

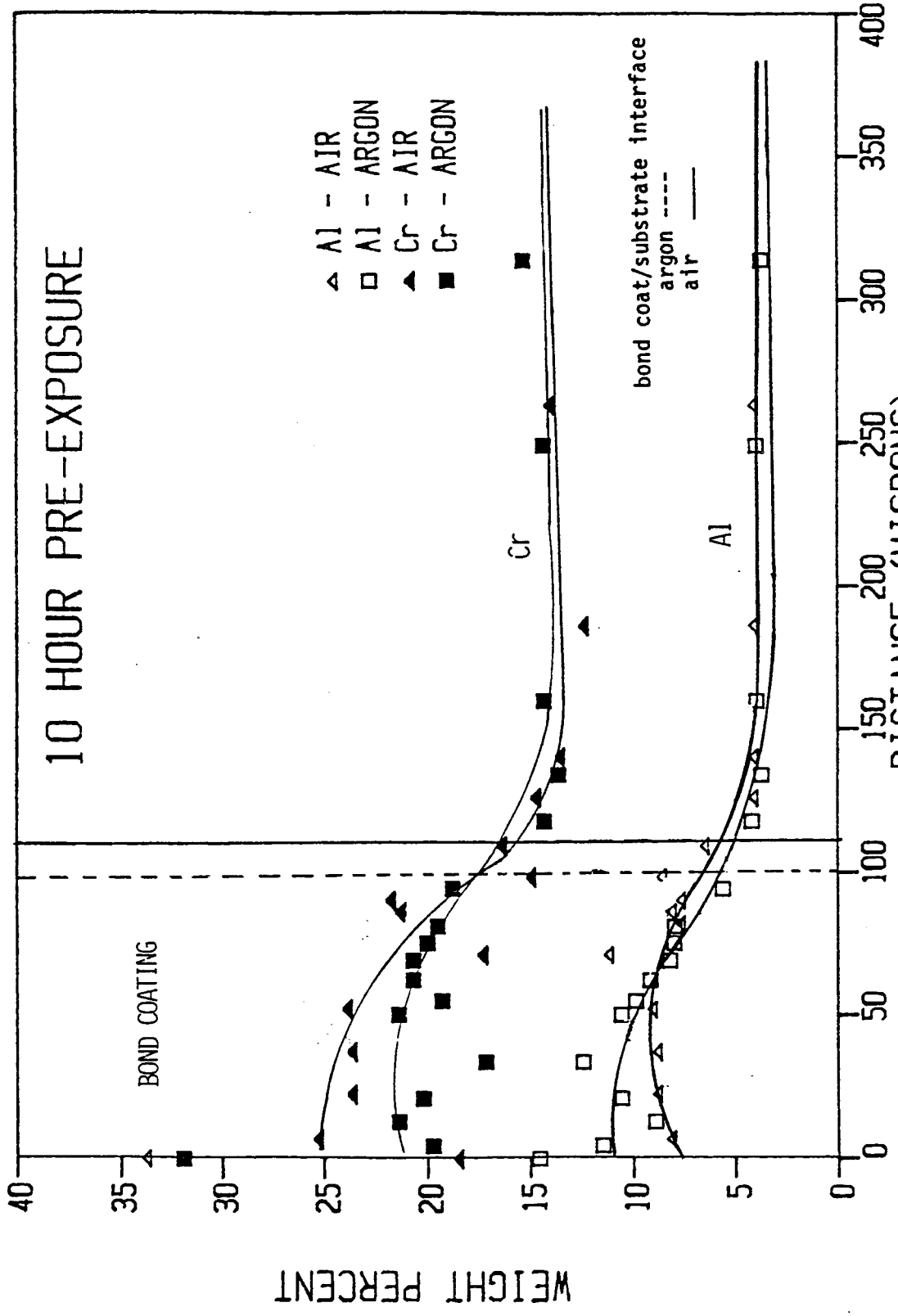

Figure 13 Bond coat - substrate concentration/distance profiles for Al and Cr
a) 10 hour pre-exposures

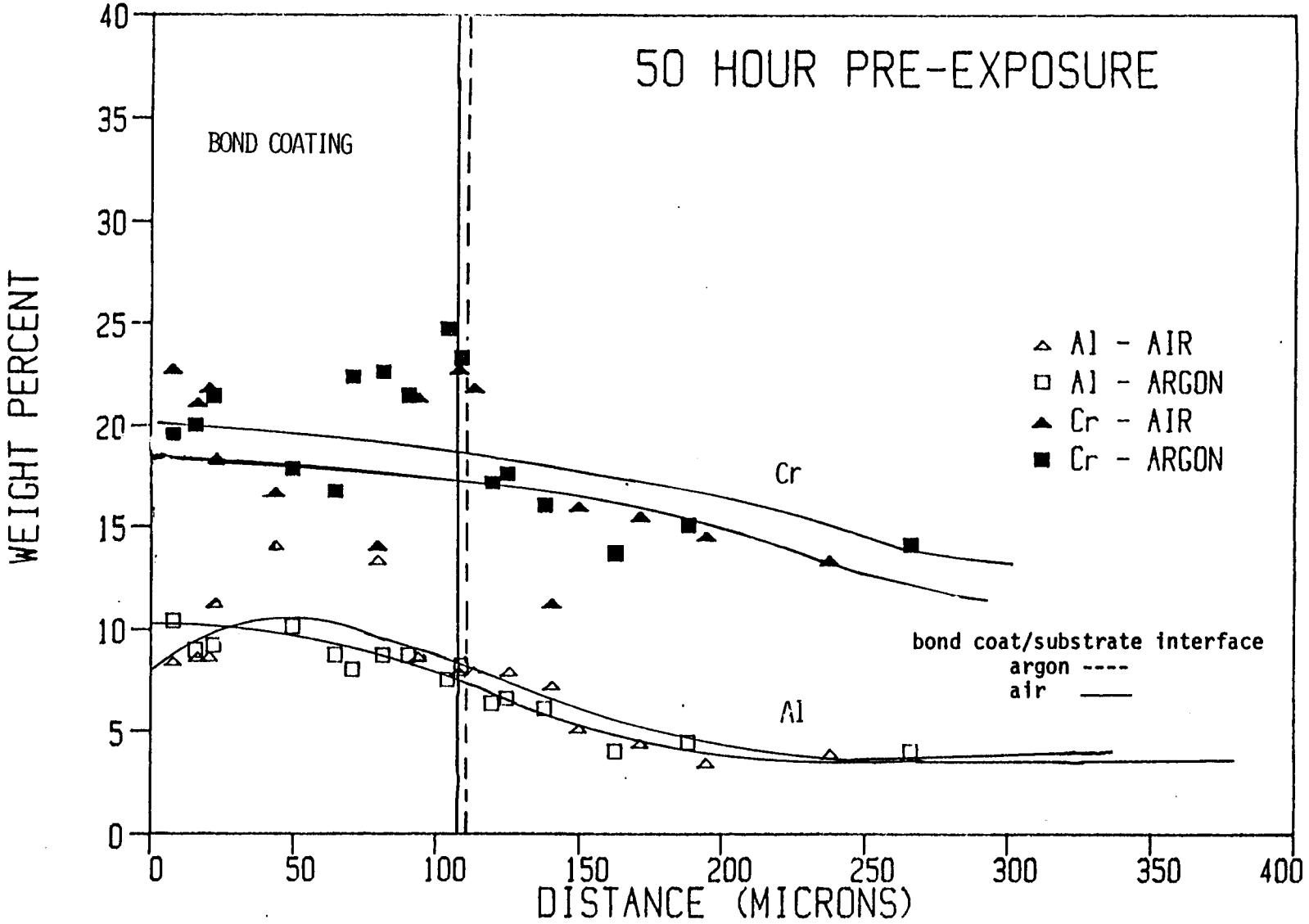

Figure 13 Bond coat - substrate concentration/distance profiles for Al and Cr
b) 50 hour pre-exposures

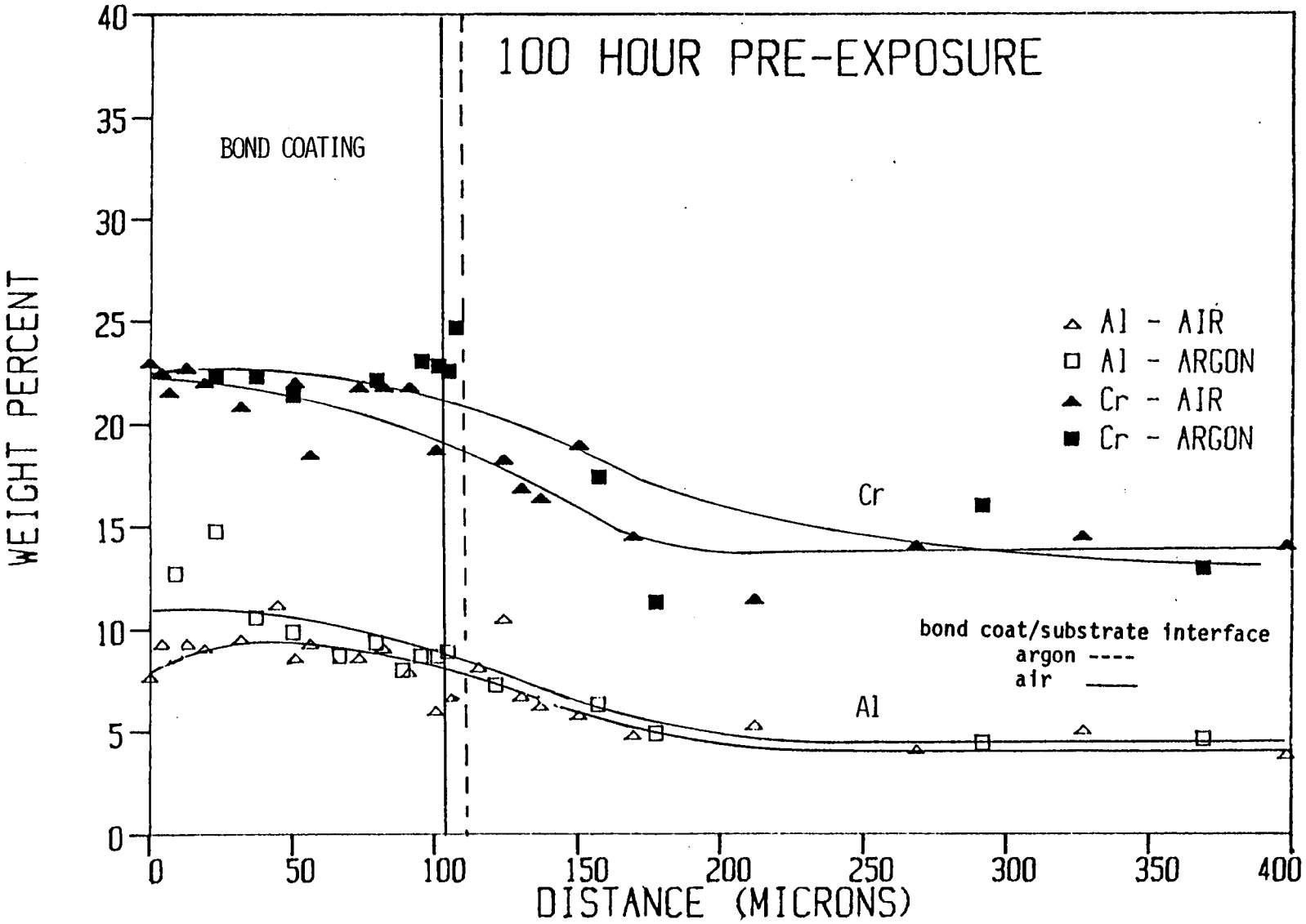

Figure 13 Bond Coat - substrate concentration/distance profiles for Al and Cr
c) 100 hour pre-exposures .

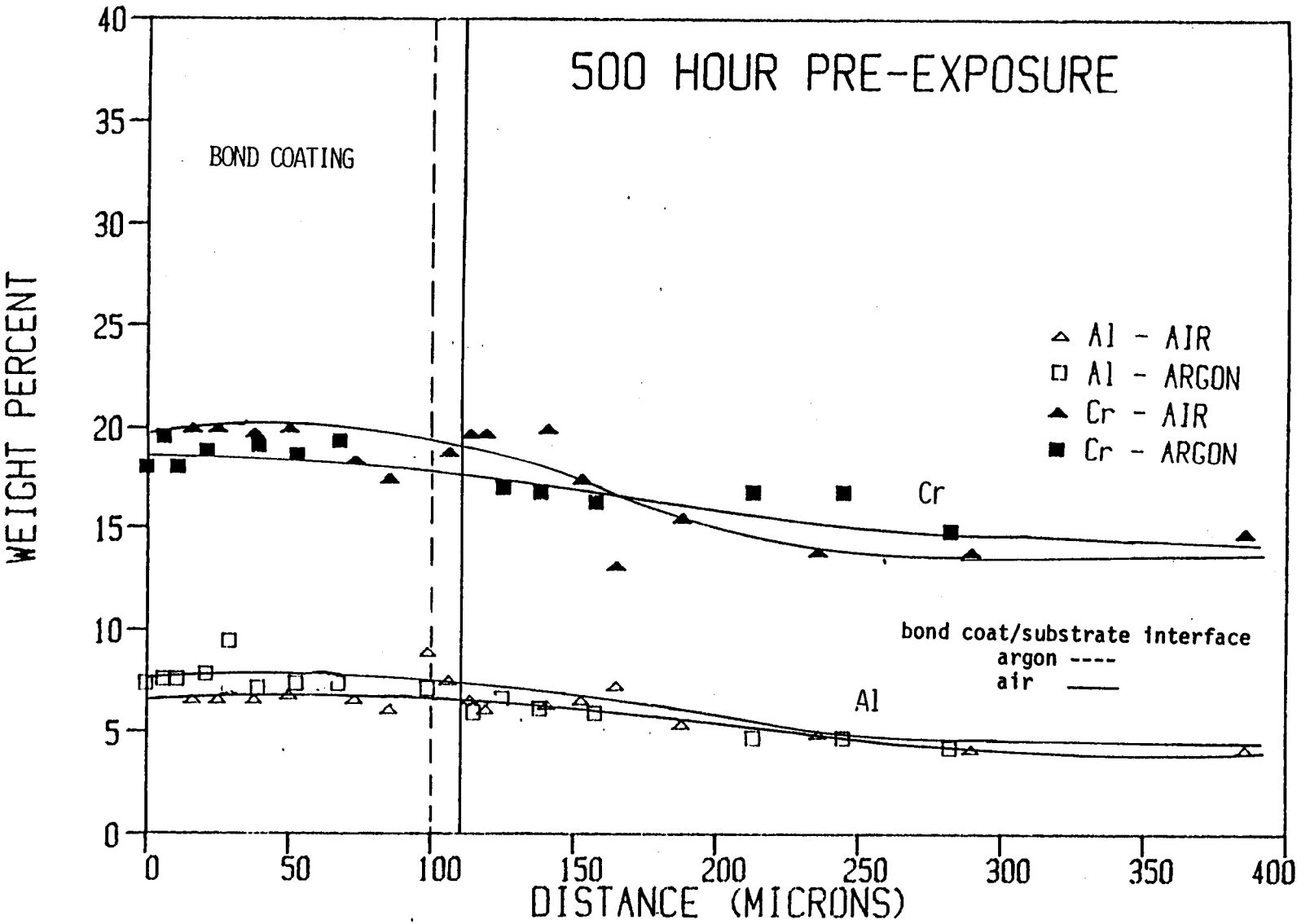

Figure 13 Bond coat - substrate concentration/distance profiles for Al and Cr
d) 500 hour pre-exposures

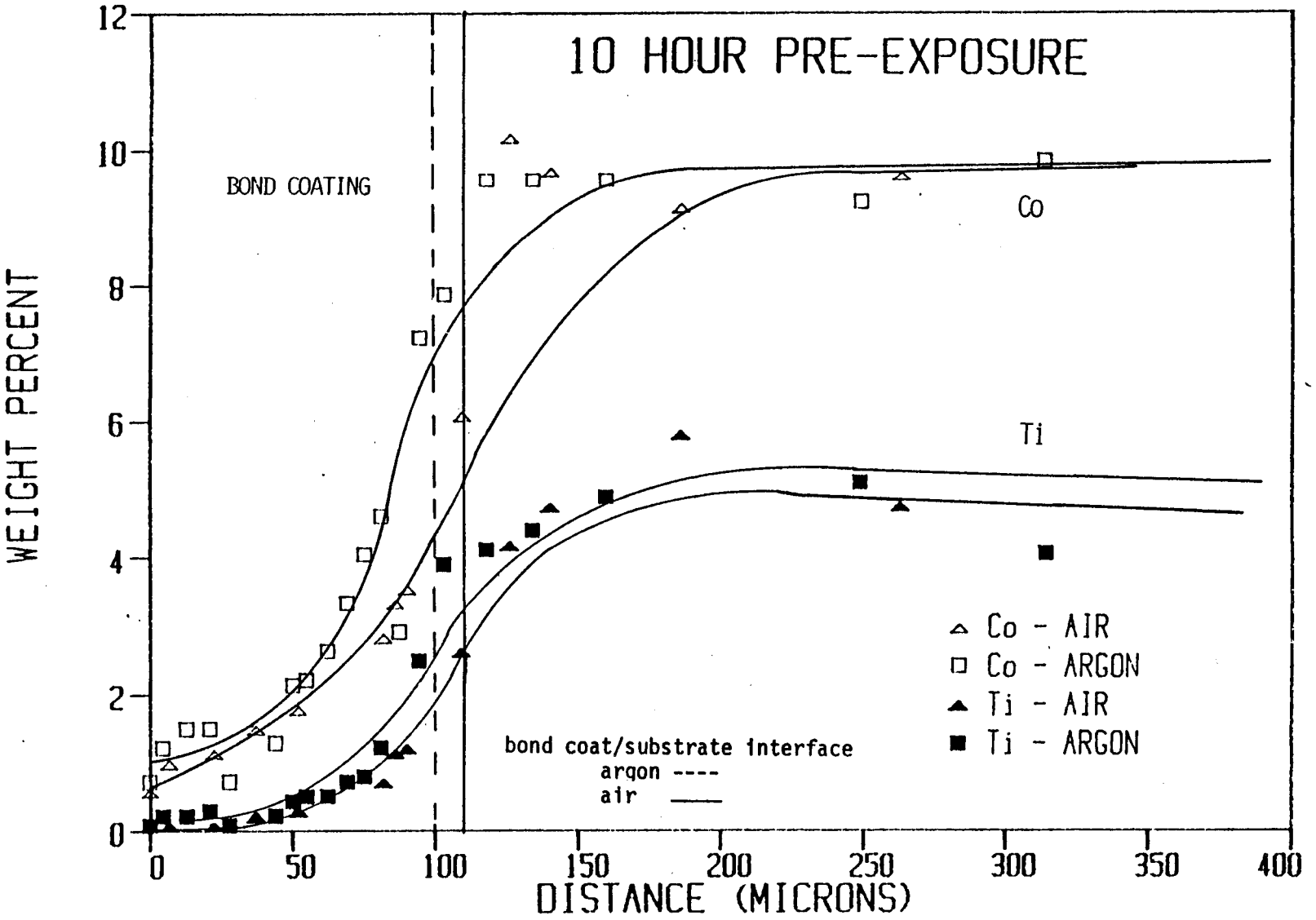

Figure 14 Bond coat - substrate concentration/distance profiles for Co and Ti
a) 10 hour pre-exposures

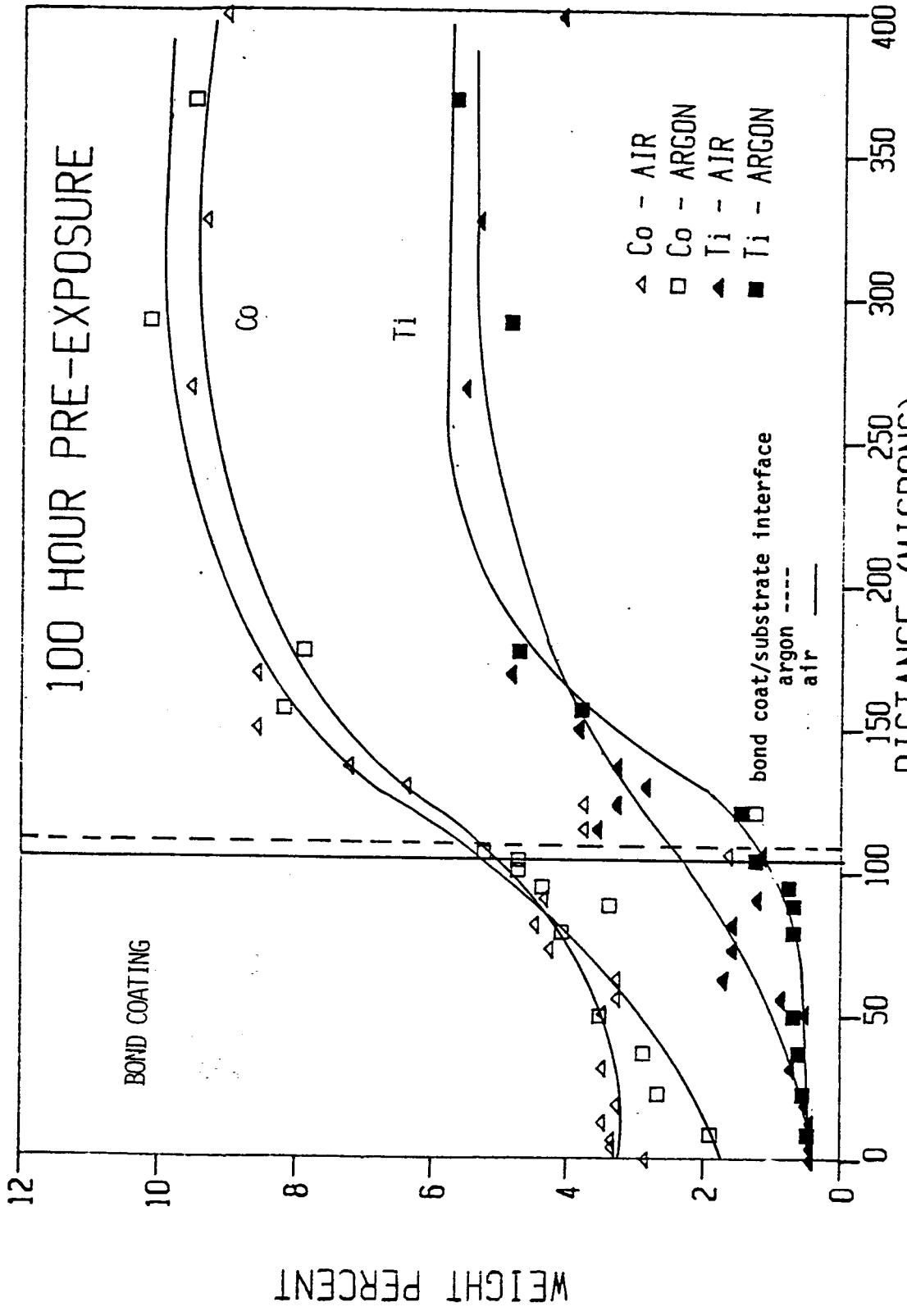

Figure 14 Bond coat - substrate concentration/distance profiles for Co and Ti
b) 100 hour pre-exposures

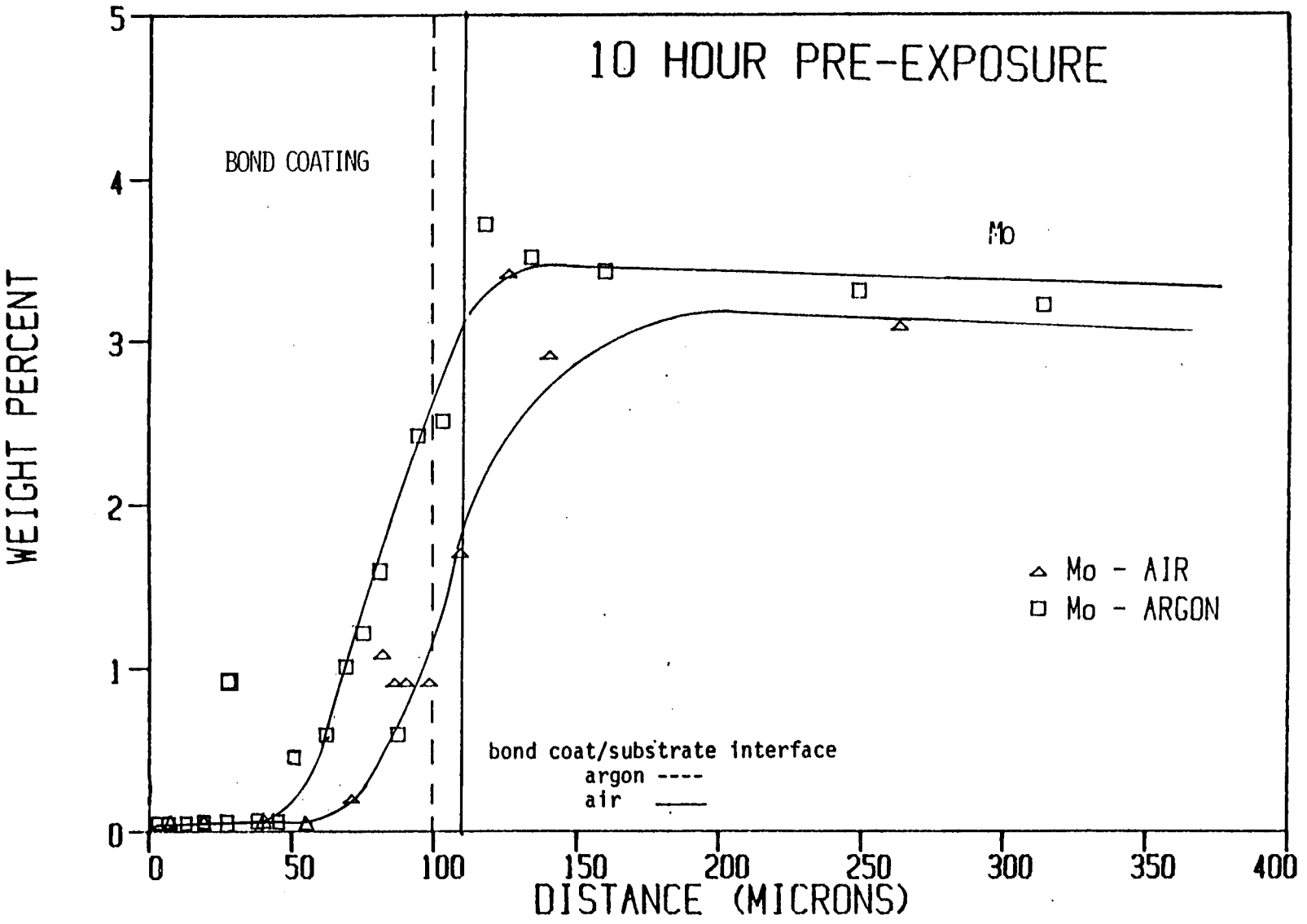

Figure 15 Bond coat - substrate concentration/distance profiles for Mo
a) 10 hour pre-exposures

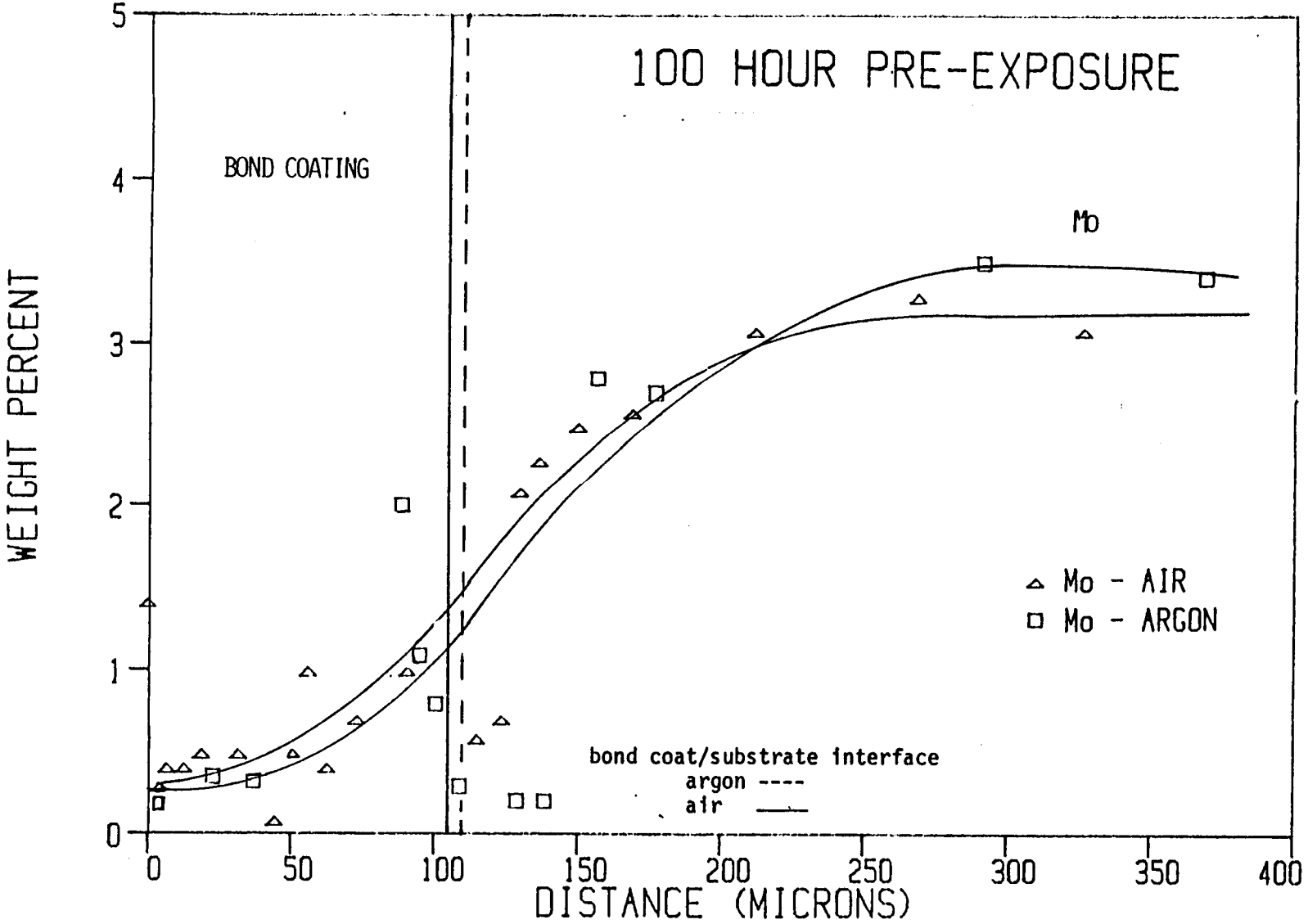

Figure 15 Bond coat - substrate concentration/distance profiles for Mo
b) 100 hour pre-exposures

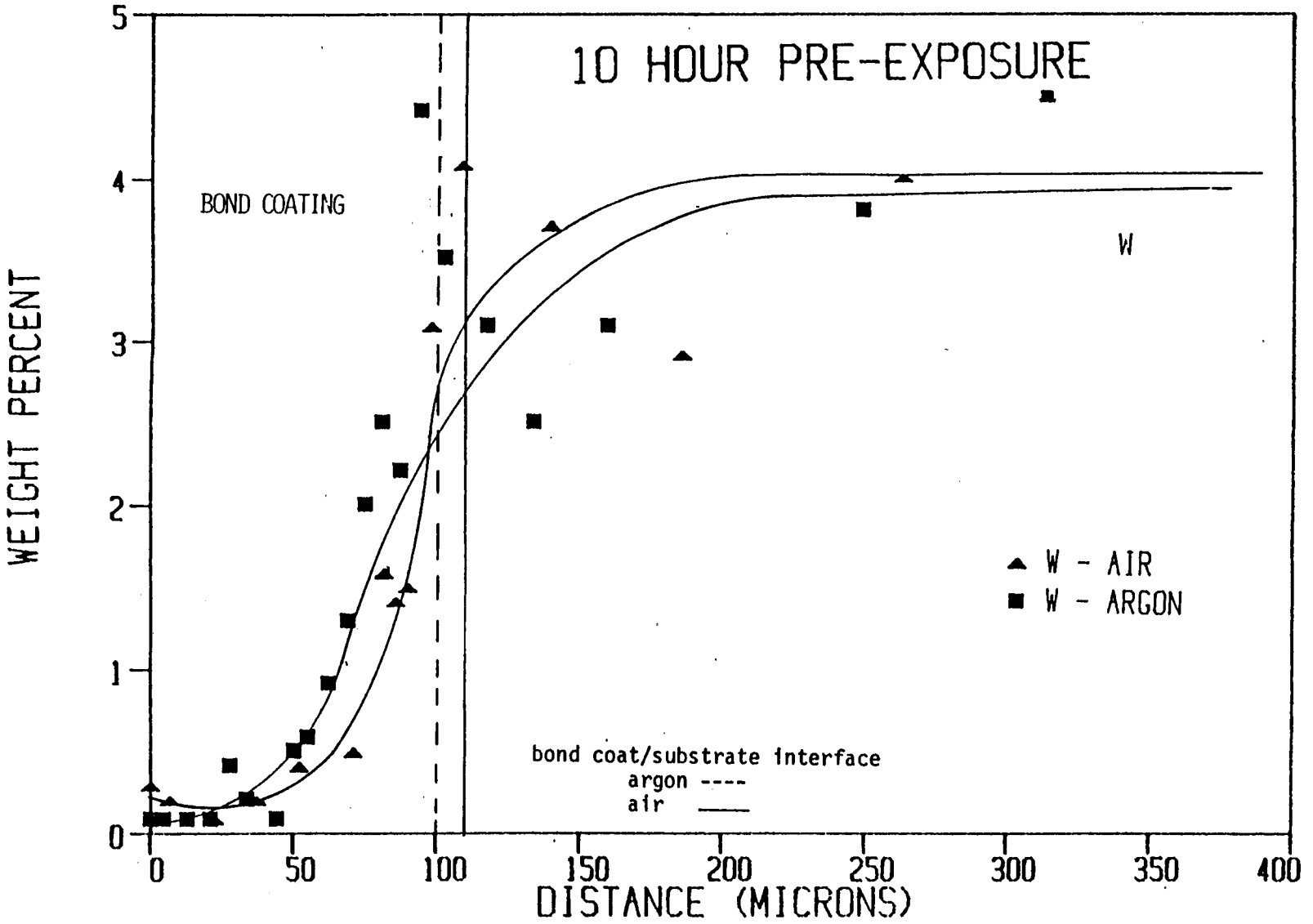

Figure 16 Bond coat - substrate concentration/distance profiles for W
a) 10 hour pre-exposures

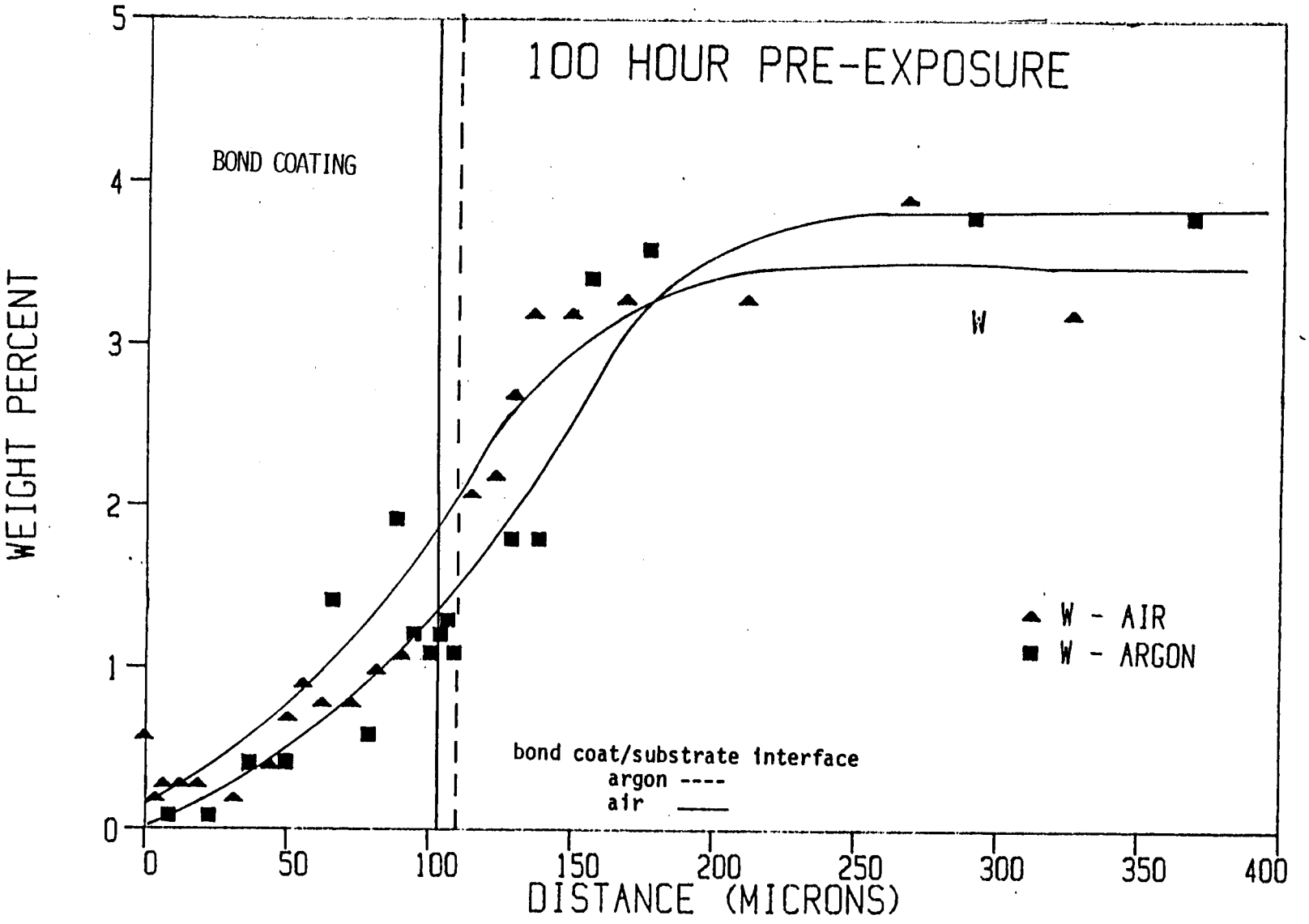

Figure 16 Bond coat - substrate concentration/distance profiles for W
b) 100 hour pre-exposures

Concentration distance/profiles on the pre-exposure specimens will also be determined for the TBC systems utilizing four different bond coats after the 100 hour pre-exposure time. These profiles were not available for this report.

These profiles combined with thermal cycle test data may indicate that composition matching of the substrate to the bond coat strongly affects TBC integrity. Possibly, compositional data may be required to model TBC systems. This situation would require a more detailed probe analysis.

Thermal Cycle Tests

Bond Coat Oxidation Effect Experiments

Thermal cycle testing in air to evaluate bond coat oxidation as a failure mechanism has been completed. In all cases, initial spalling occurred at the top coat edges (Figure 17). However, in some cases catastrophic failure (complete spalling) of the TBC occurred (Figure 17). Failure was defined as when 10% (surface area) of the ceramic top coat had spalled.

Unexpectedly, the specimen pre-exposed in argon failed before the specimens pre-exposed in air (Figures 18, 19). Failures in all cases occurred in the ceramic top coat (Figure 20) approximately 0.025 - 0.050 mm (.001 - .002") from the bond coat/top coat interface (normal TBC failure location). Continuous oxide scales of 3-4 μm (excluding the 472 hour pre-exposure (Table VIII and Figures 21, 22) were observed at the bond coat/top coat interface for the as-sprayed and air pre-exposed specimens after thermal cycle testing at failure. This is contrasted with the specimens pre-exposed in argon where oxide scales generally less than 1 μm developed and appeared non-continuous by optical microscopy (Figures 23, 24) after thermal cycle testing.

Figure 17 Failed TBC specimens after thermal cycle testing in air

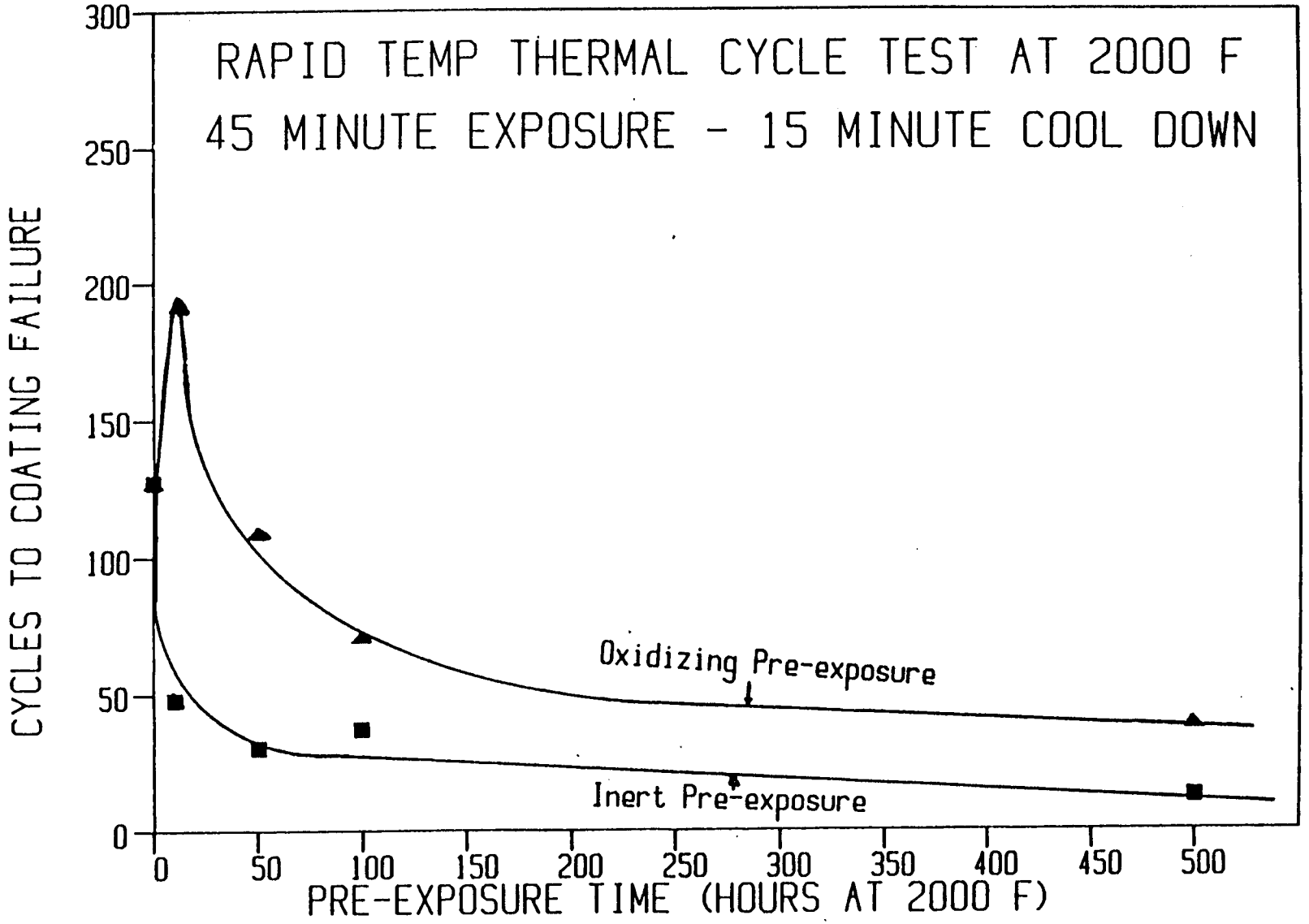

Figure 18 Test results for thermal cycle testing in air for bond coat oxidation effect specimens (values plotted are average of three test specimens)

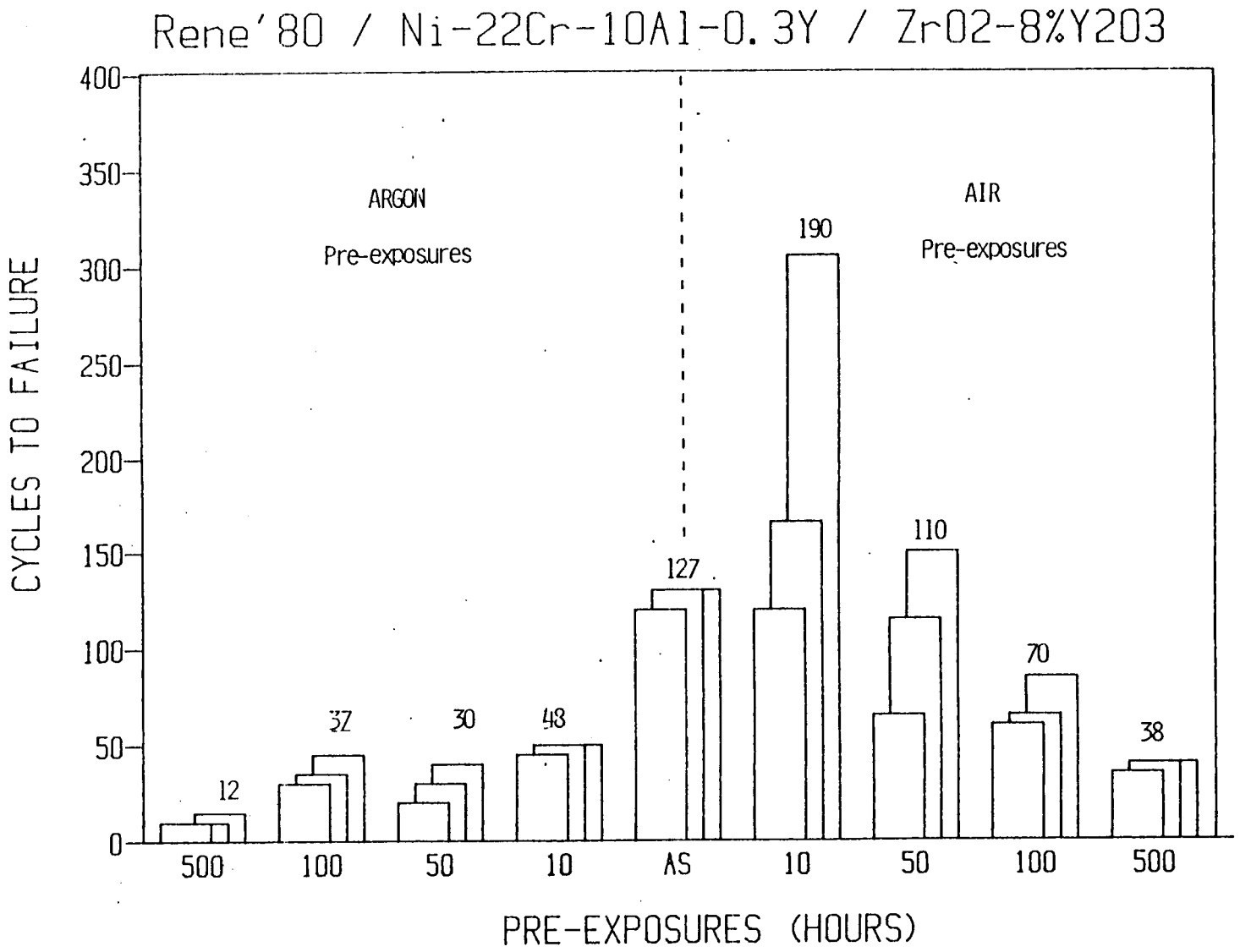

Figure 19 Test results for thermal cycle testing in air for bond coat oxidation specimens (values plotted for each individual specimen).

TABLE VIII OXIDE SCALE THICKNESS OF FAILED BOND COAT OXIDATION EFFECT SPECIMENS (average value of three test specimens) AFTER THERMAL CYCLING

Pre-exposure Condition*	Oxide Scale Thickness(μms)
As-Sprayed	3.6
10 hour air	4.0
50 hour air	3.6
100 hour air	4.0
500 hour air	6.7

*Specimens pre-exposed in argon had scales less than 1 μm thick.

a) 100 hour argon pre-exposure
(50 cycles)

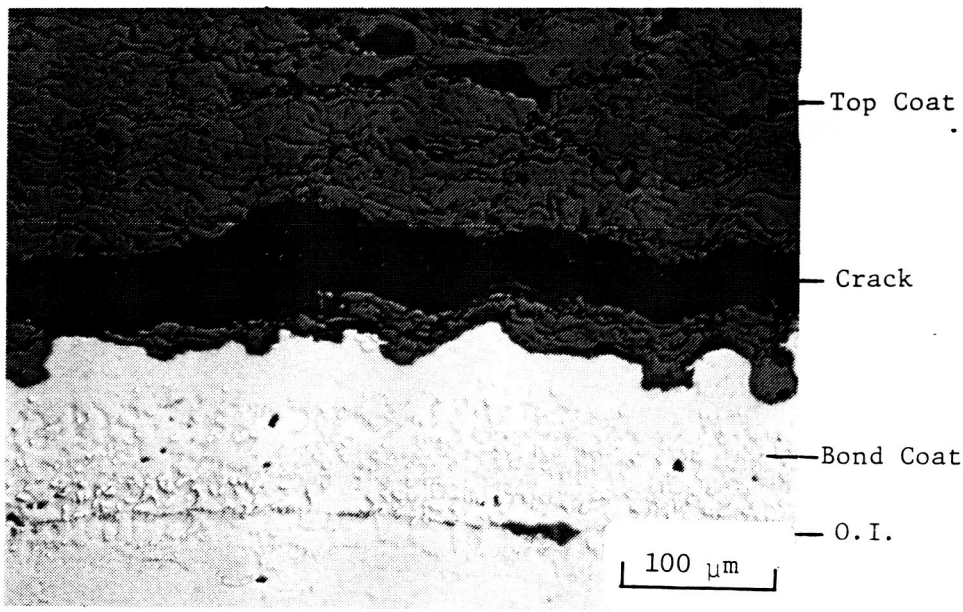

b) 100 hour air pre-exposure
(65 cycles)

Figure 20 Microstructure of TBC at failure location after thermal cycle testing

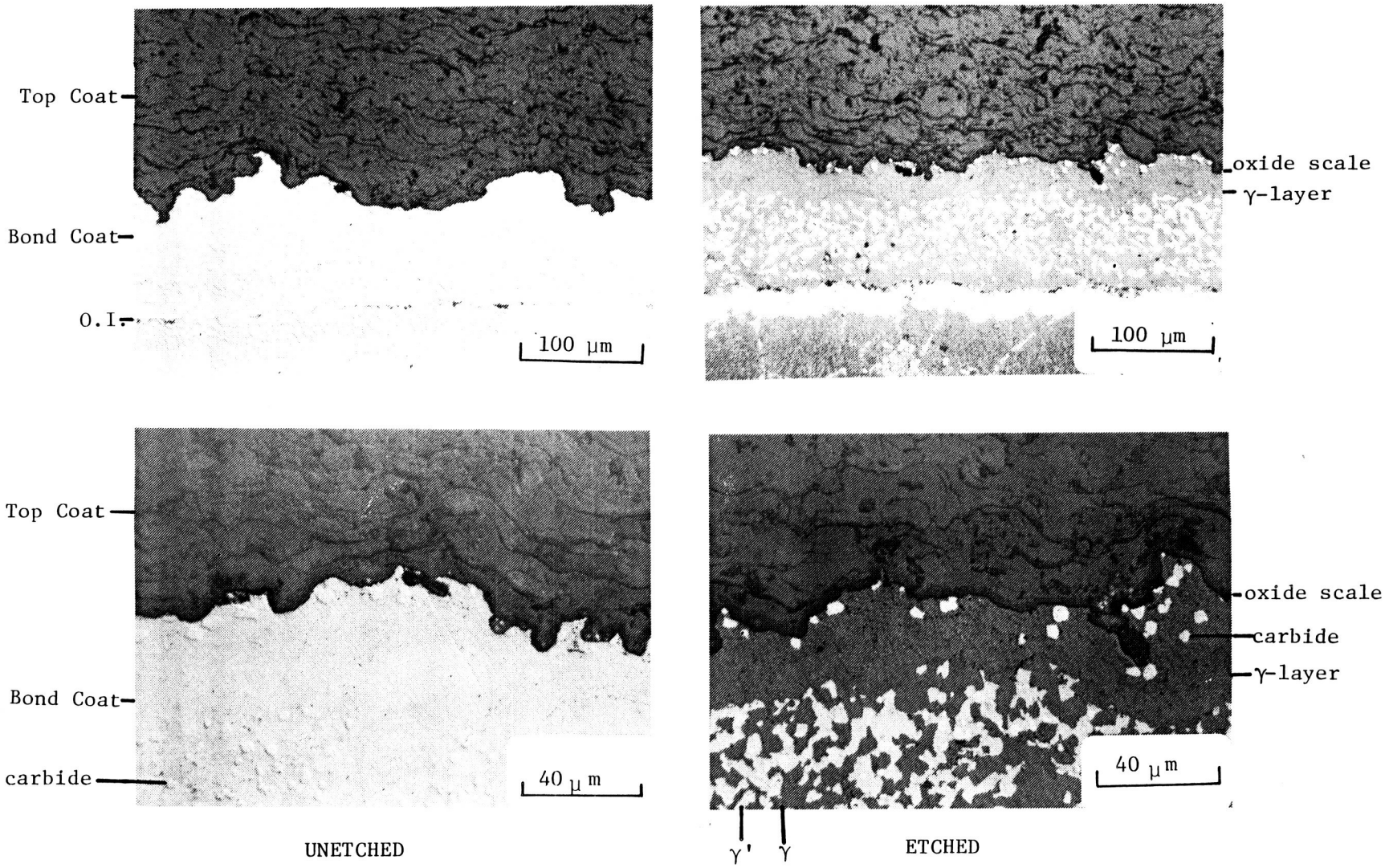

Figure 21 Microstructure after failure of specimen without pre-exposure (130 cycles)

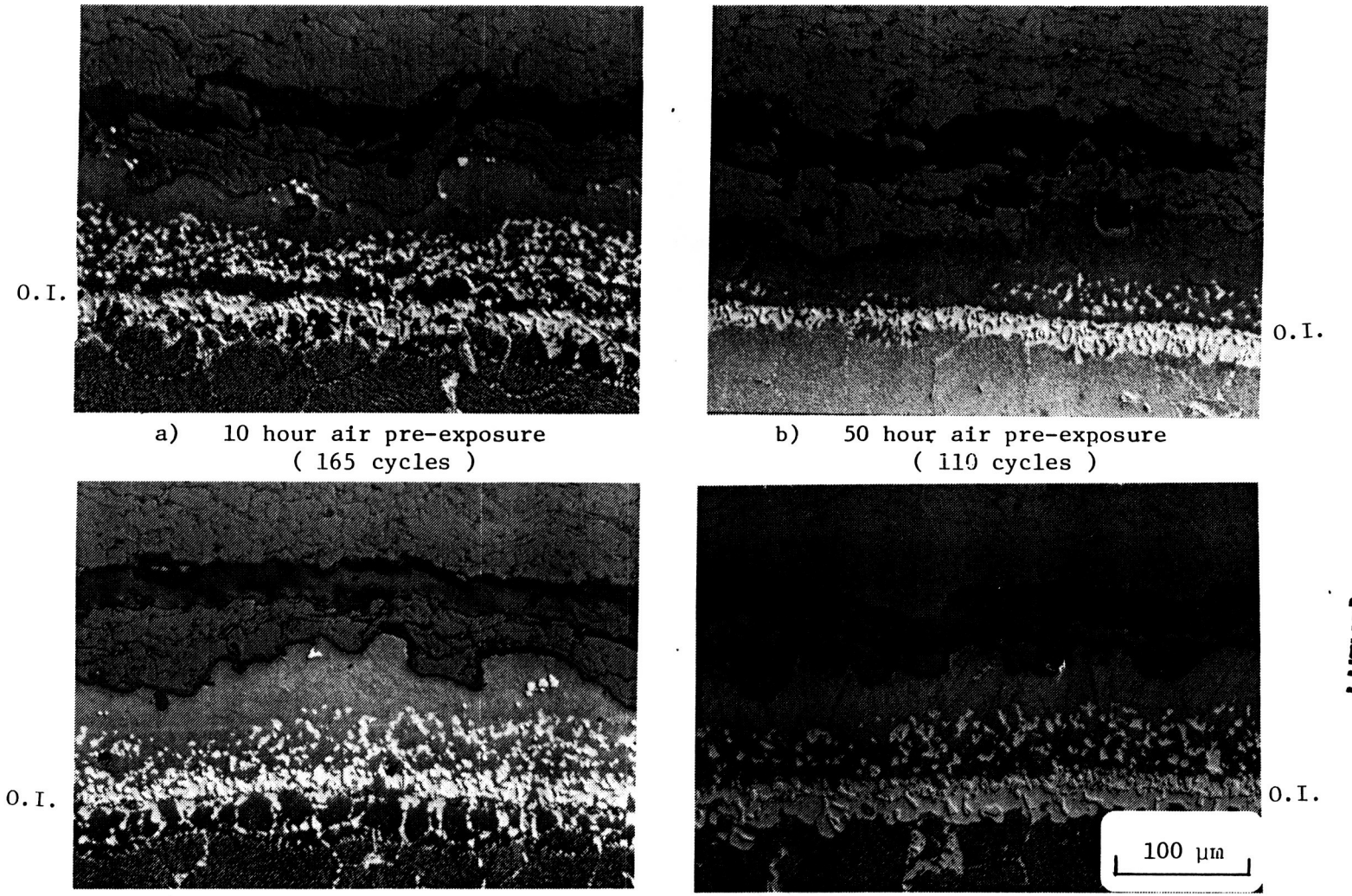

a) 10 hour air pre-exposure (165 cycles)

b) 50 hour air pre-exposure (110 cycles)

c) 100 hour air pre-exposure (65 cycles)

d) 472 hour air pre-exposure (40 cycles)

ETCHED

Figure 22 Microstructures of air pre-exposed specimens after thermal cycle testing

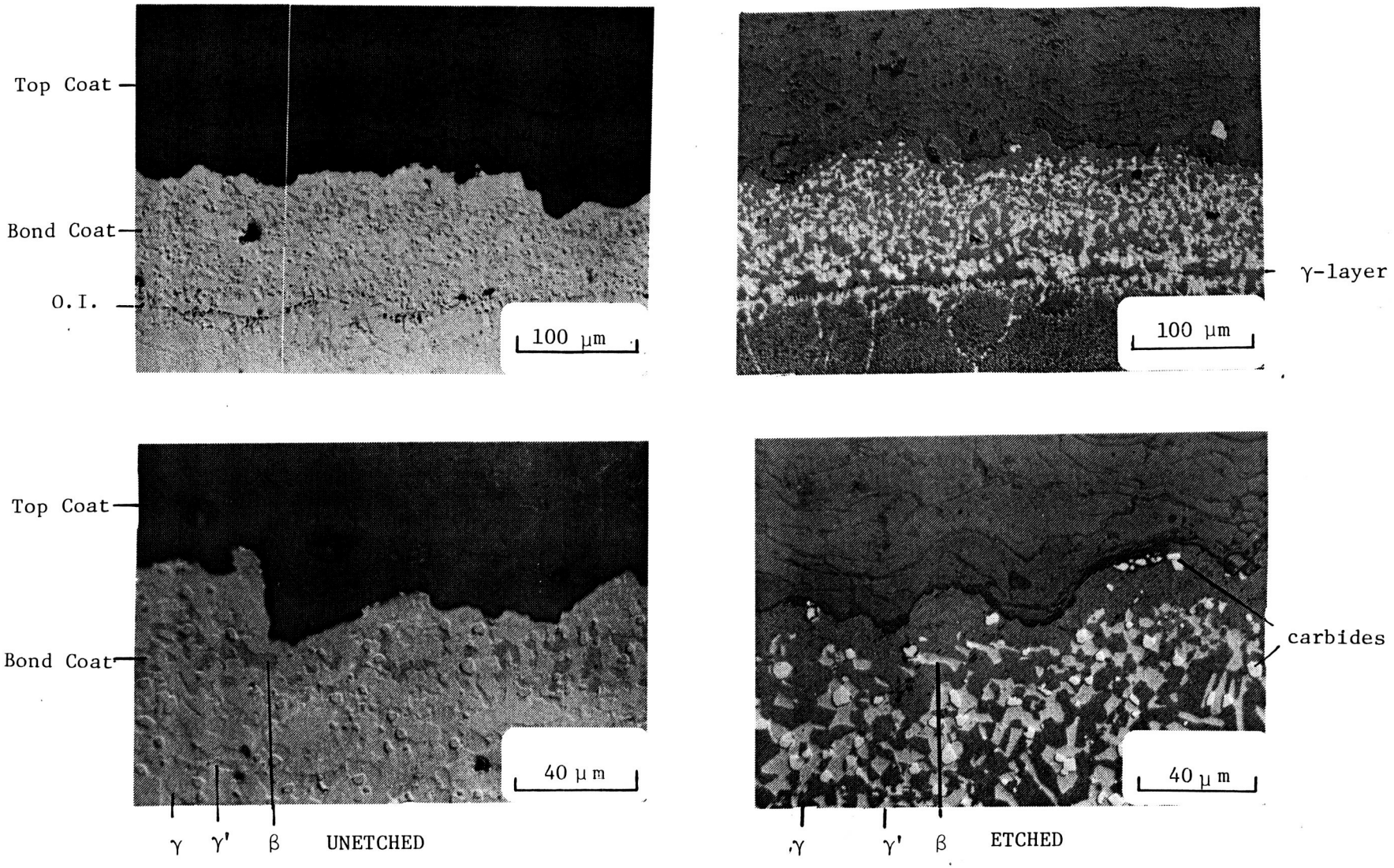

Figure 23 Microstructure of 50 hour argon pre-exposed specimen after thermal cycle testing (20 cycles)

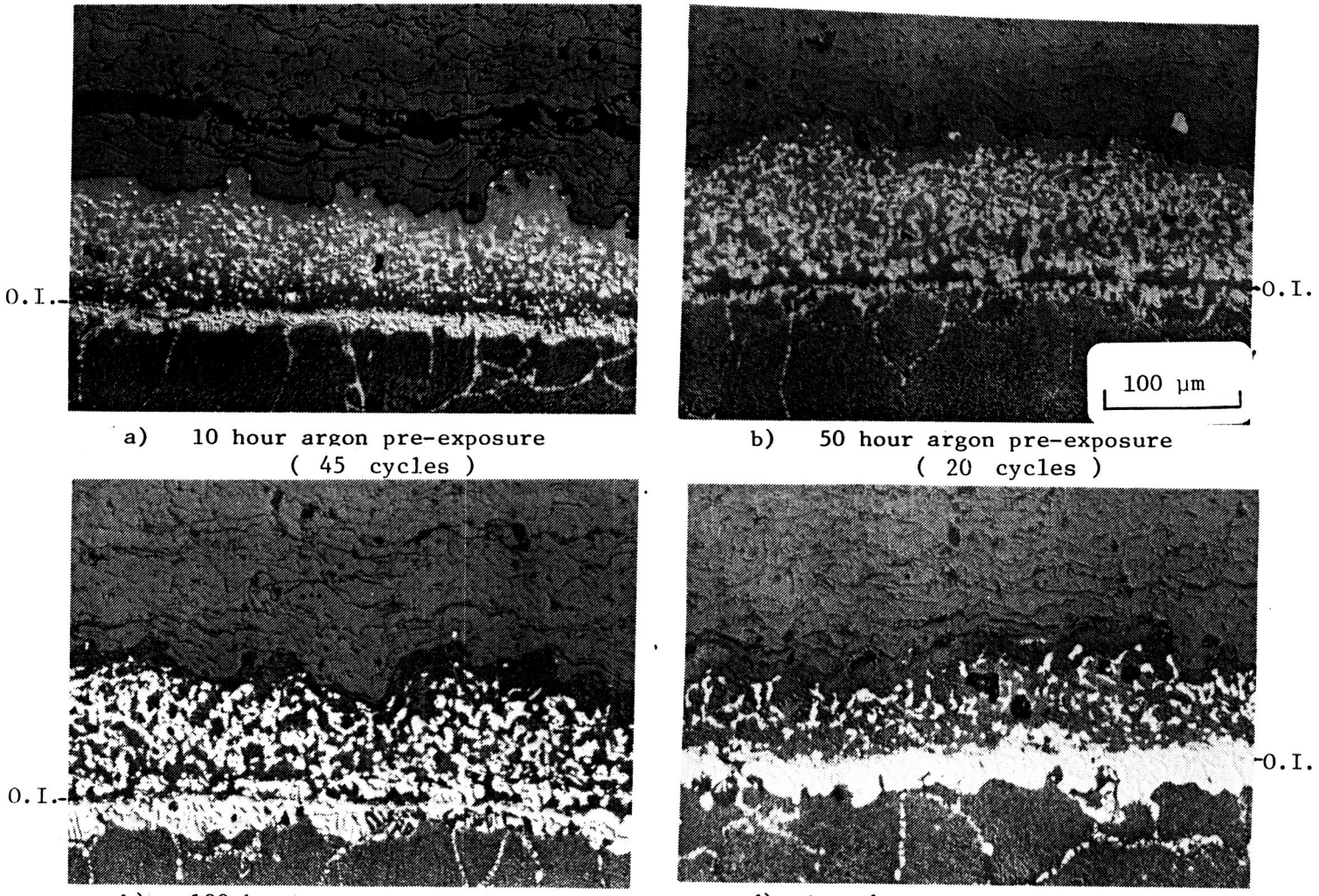

a) 10 hour argon pre-exposure (45 cycles)

b) 50 hour argon pre-exposure (20 cycles)

b) 100 hour argon pre-exposure (50 cycles)

d) 472 hour argon pre-exposure (10 cycles)

ETCHED

Figure 24 Microstructures of argon pre-exposed specimens after thermal cycle testing

Investigations are underway to try to understand this unexpected result. These investigations include X-ray diffraction, metallography, micro-hardness, electron microprobe, and scanning electron microscope analysis.

Another interesting result was the improved thermal cycle life for the specimens pre-exposed in air for 10 hours. A possible explanation is that the improvement can be attributed to the improved bond coat/top coat adherence associated with the Al_2O_3 scale that is present before thermal cycling. Generally, in the as-sprayed condition, the bonding between the ceramic top coat and metal bond coat is considered essentially mechanical. The mechanical nature of this bond is demonstrated by the bond coat surface roughness requirement. However, the growth of the continuous Al_2O_3 scale during the air pre-exposure should increase the chemical bond between the bond coat and the top coat. The improved adherence may override the negative effects produced by the stresses developed due to the addition of the Al_2O_3 scale (constraint stresses). Also, initial Al_2O_3 growth may not develop these constraint stresses. Bond coat and top coat sintering during the pre-exposure may allow the growth of small quantities of scale before stresses are developed. This result will be further evaluated.

Generally, good repeatability (thermal cycle lives) was observed for each pre-exposure condition. The exceptions were the 10 and 50 hour air pre-exposures where significant scatter was observed from one specimen to another (Figure 19). Investigations are underway to correlate the differences to microstructure and processing history.

Thermal cycle testing in argon to further evaluate bond coat oxidation as a failure mechanism has not yet started. The specimens are presently in the

as-sprayed condition, but the pre-exposures in air and argon have been delayed until the cause of the unexpected result in the above experiment can be further assessed.

Bond Coat Creep Effect Experiments

The specimens for evaluating the effect of bond coat creep on TBC failure have received both the air and argon pre-exposures. These specimens will be used to evaluate the effect of bond coat creep, and also will evaluate how these pre-exposures affect TBCs with high strength bond coats. Thermal cycle tests in air of these specimens have also been initiated.

Key Property Determination

The procedures to determine tensile strength, Poisson's ratio, dynamic modulus, and coefficient of thermal expansion have been finalized. These properties will be determined for both the bond coat and the top coat at room temperature (RT), 538°C (1000°F), 982°C (1800°F), 1038°C (1900°F), and 1093°C (2000°F).

Standard testing procedures and test specimens (Figure 25) will be utilized for the NiCrAlY bond coat specimens. These specimens will be machined from 5.1 cm (wide) by 15.2 cm (length) heat treated LPPS NiCrAlY billets (various heights). The as-sprayed billets will receive a four hour vacuum heat treatment at 1093°C (2000°F). The heat treatment is used to increase the machinability of the billets. The 1093°C heat treatment temperature was chosen since this is the soak temperature utilized in thermal cycle testing.

Special test configurations (Figure 26) will be required for the ceramic top coat specimens. In all tests, free-standing air plasma sprayed (APS)

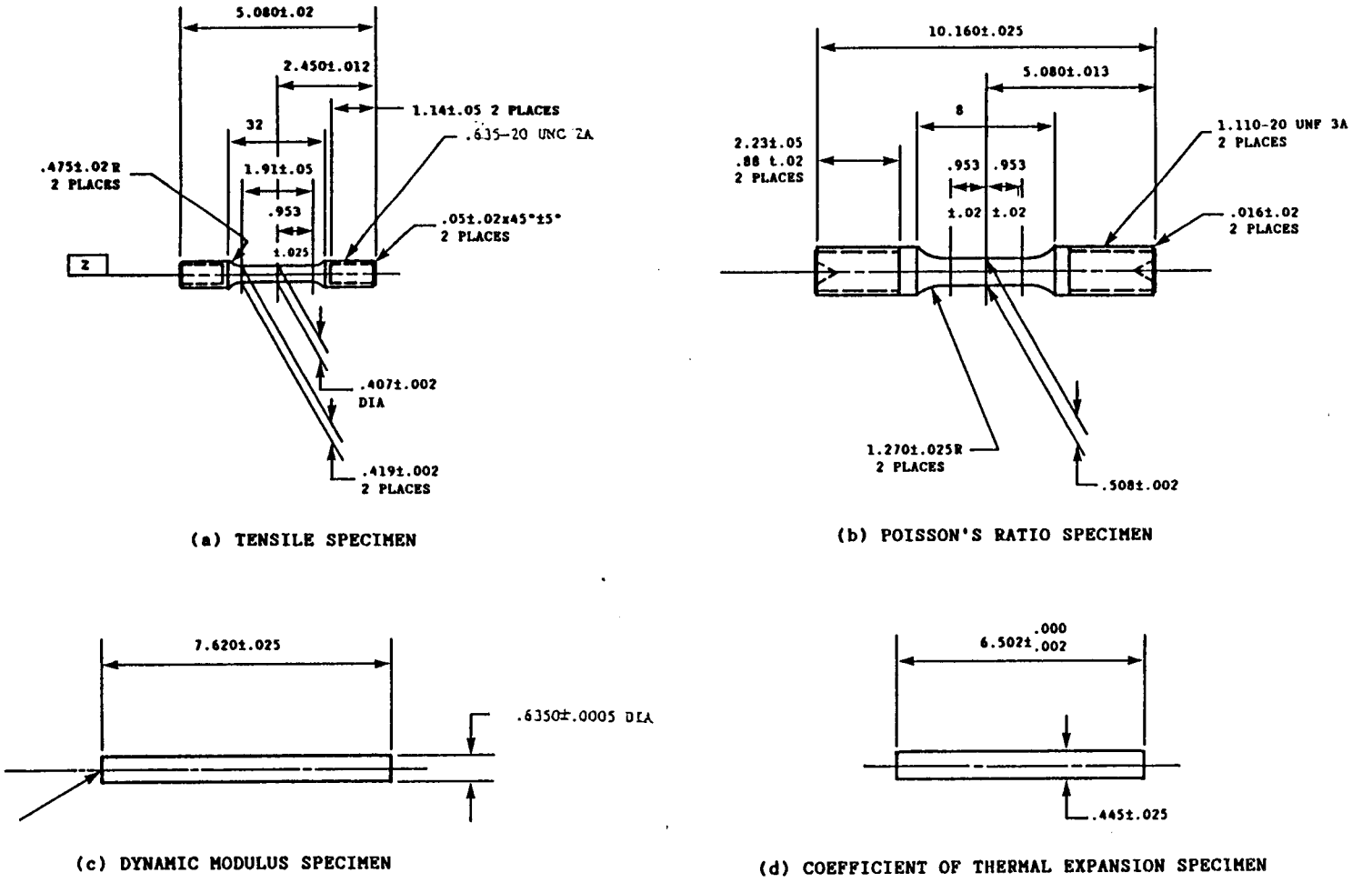

Figure 25 Bond coat specimen configurations (all dimensions in centimeters)

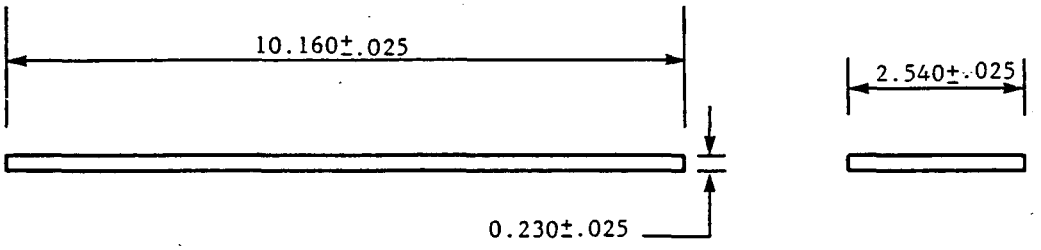

(a) DYNAMIC MODULUS AND POISSON'S RATIO SPECIMEN.

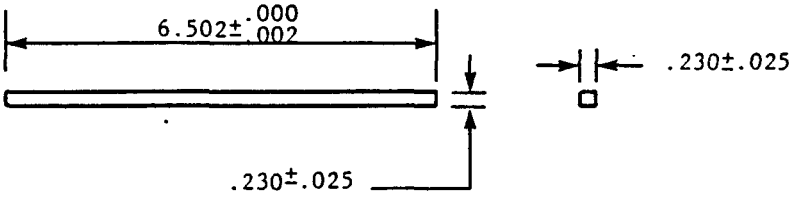

(b) COEFFICIENT OF THERMAL EXPANSION SPECIMEN

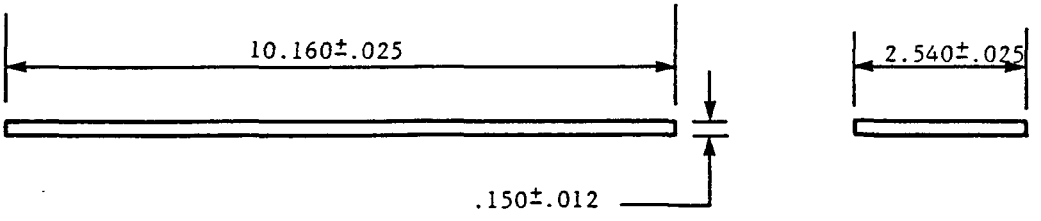

(c) BEND STRENGTH SPECIMEN

Figure 26 Top coat specimen configurations (all dimensions in centimeters)

specimens will be utilized. Free-standing specimens will be produced by depositing the ceramic coating material on copper or stainless steel substrates and inducing a thermal shock to cause spallation of the intact ceramic sheet. Some final machining may be required to achieve the desired specimen configurations (Figure 26). These specimens will receive a four hour heat treatment in air at 1093°C (2000°F) prior to testing.

Special testing procedures will also be required for the top coat specimens. Bend strength will be determined utilizing the four point bend test. Poisson's ratio will be determined utilizing two different methods. In the first method, strain gauges will be attached to bend test specimens. This method (limited to room temperature) has previously been utilized to determine Poisson's ratio at RT for free standing APS $MgO-ZrO_2$ specimens (5). Poisson's ratio will also be determined at RT and elevated temperatures by resonance techniques. In this technique, Poisson's ratio will be calculated from the shear modulus and dynamic modulus measurement obtained by this technique. Finally, coefficient of thermal expansion will be measured utilizing the Chevenard dilatometer.

CONCLUSIONS

The first task of the study involves the determination of TBC failure mechanisms. The information will be utilized in conjunction with key property determination and thermomechanical testing results to develop TBC life prediction models.

Thermal cycle testing in air to evaluate oxidation as a failure mechanism has been completed. Inert pre-exposures in argon have been very effective in reducing bond coat oxidation. Unexpectedly, initial test data indicate that pre-exposures in argon are more detrimental to thermal cycle life (shorter thermal cycle life) than pre-exposures in air. The lower thermal cycle life may be attributed to less adherence of the top coat to the bond coat in specimens that were pre-exposed in argon. Investigations are underway to test this hypothesis and evaluate other possibilities. Thermal cycle tests in argon have been delayed until the cause of this result is more completely understood. Additional experiments are also being considered to supplement the pre-exposure experiments being utilized to evaluate bond coat oxidation as a failure mechanism.

The specimens to be used for evaluating the effect of bond coat creep strength on TBC thermal cycle life have received a 100 hour pre-exposures in air or argon, or no pre-exposure. Thermal cycle testing of these specimens in air has been initiated. The test will evaluate the effect of bond coat creep and also test the repeatability of the detrimental effects of argon pre-exposures on different TBC systems (different bond coats).

Finally, key property determination methods for the bond coat and top coat have been selected. The properties will be determined in the second year of this project.

REFERENCES

1. Busch R., "Develop Sputter Deposited, Graded Metal ZrO_2 Coating Technology for Application to Turbine Hot Section Components," Naval Sea System Command # N00024-75-C-4333, 1976.

2. Duderstadt, E.C. and Agarwal, P., "Energy Efficient Engine - High Pressure Turbine Thermal Barrier Coating Support Technology Report, " General Electric Company, Aircraft Engine Business Group, R82AEB293, NASA CR-168037, 1982.

3. Stecura, S. "Effects of Yttrium, Aluminum, and Chromium Concentrations in Bond Coatings on the Performance of Zirconia - Yttria Thermal Barriers," NASA TM-79206, 1979.

4. Gedwill, M.A., "Improved Bond Coatings for Use with Thermal Barrier Coatings," NASA TM-81567, 1980.

5. Miller, R.A. and Lowell, C.E., "Failure Mechanisms of Thermal Barrier Coatings Exposed to Elevated Temperatures", NASA TM-82905, 1982.

6. Miller, R.A. and Berndt, C.C., "Performance of Thermal Barrier Coatings in High Heat Flux Environments," NASA TM-83663, 1984.

7. 1982 Independent Research and Development Technical Plan, General Electric Company, Aircraft Engine Business Group, R82AEB244, Vol. V, 1982.

8. Stecura, S. "Optimization of the NiCrAlY/ZrO_2-Y_2O_3 Thermal Barrier System, " NASA TM-86905, 1985.

9. Miller, R.A. "Oxidation Behavior of a Thermal Barrier Coating," Proceeding on High Temperature Protective Coating, edited by S.C. Singhal, Presented at 112th AIME Annual Meeting, Atlanta, Georgia, March 7-8, 1983.

10. Miller, R.A., Agarwal, P., and Duderstadt, E.C.,"Life Modelling of Atmospheric and Low Pressure Plasma Sprayed Thermal Barrier Coatings, " Presented at 1984 American Ceramic Society Meeting , Cocoa Beach, Florida, 1984.

11. Miller, R.A., "Oxidation - Based Model for Thermal Barrier Coating Life," Ceramic Journal, p. 83, August, 1984.

12. 1984 Independent Research and Development Technical Plan, General Electric Company, Aircraft Engine Business Group, R84AEB454, Project 10.18, 1984.

13. Valentine, P.G. and Maier, R.D., "Microstructure and Mechanical Properties of Bulk and Plasma - Sprayed Y_2O_3 - Partially Stabilized Zirconia", NASA CR-165126, 1980.

14. Gill, B.J., "Plasma deposited MCrAlY and thermal barrier coatings for gas turbine components," Presented at First Conference On Material Engineering, ME, 10-12 July 1984.

15. Stecura, S. "Effects of Compositional Changes On The Performance Of A Thermal Barrier Coating System," NASA TM 78976, 1979.

16. Miller, R.A., Garlick, R.G., and Smialek, J.L., "Phase Distributions in Plasma Sprayed Zirconia - Yttria," American Ceramic Society Bulletin, V.62, p. 1355-1358, Dec., 1983.

17. Agarwal, P., GE-AEBG, unpublished data, 1983.

18. Anderson, C.A. and Gupta, T.K., "Phase stability and transformation toughening in zirconia", Science And Technology Of Zirconia, Advances In Ceramics, Vol.3, edited by Heuer, A.H. and Hobbs, L.W. , American Ceramics Society, p. 184, 1981.

19. Evans, A..G., "Toughening Mechanisms in Zirconia Alloys," Science And Technology Of Zirconia II, Advances In Ceramics, Vol. 12, edited Heuer, A.G., Claussen, N., and Ruhle, M., American Ceramic Society, p. 193, 1984.

20. Valentine, P.G. , Maier, R.D., and Mitchell, T.E., "Microstructure and Mechanical Properties of Bulk Yttria - Partially - Stabilized Zirconia", NASA CR-165402, 1981.

21. Mantkowski, T.E., Rigney, D.V., Froning, M.J., and Jayaraman, N., "Characterization of ZrO_2 - Y_2O_3 Thermal Spray Powder Systems," Presented at NASA Thermal Barrier Coating Workshop, May 21, 22 1985, Cleveland, Ohio.

22. Hendricks, R.C., and McDonald, G., "Effects of Arc Current on the Life in Burner-Rig Thermal Cycling of Plasma - Sprayed ZrO_2 - Y_2O_3", Ceramic Engineering Society Proceeding, Vol. 3, 1982.

23. Rangaswamy, S., and Herman, H., "Thermal Expansion Study of Plasma - Sprayed Oxide Coatings", Thin Solid Films, Vol. 73, p.43-52, 1980.

24. Cassenti, B.M., Brickley, A.M., and Sinko, G.C., "Thermal and Stress Analysis of Thermal Barrier Coatings", AIAA/SAE/ASME 17th Joint Propulsion Conference, 1981, Colorado Springs Co., AIAA-81-1482.

25. Shankar, N.R., Berndt, C.C., Herman, H., and Rangaswamy, S., "Acoustic Emission from Thermally Cycled Plasma-Sprayed Oxides", American Society Bulletin, Vo.62, No.5, May 1983.

26. Becher, P.F., Rice, R.W., Wu, C.C., and Jones, R.L., "Factors In The Degradation Of Ceramic Coatings For Turbine Alloys", Thin Solid Films, Vol. 53, p. 225-232, 1978.

27. McDonald, G. and Hendricks, R.C., "Effect Of Thermal Cycling On ZrO_2-Y_2O_3 Thermal Barrier Coatings", NASA TM-81480, 1980.

28. Bill, R.C., "A Sputtered Zirconia Primer for Improved Thermal Shock Resistance", NASA TM-81732, 1981.

29. Mullen, R.L., McDonald, G., Hendricks, R.C., and Hofle, M.M., "Correlation of Compressive Stress with Spalling of Plasma Sprayed Ceramic Materials, NASA TM-83406, 1983.

30. Watson, J.W., and Levine, S.R., "Deposition Stress Effects on Thermal Barrier Coating Burner Rig Life", NASA TM 83670, 1984.

31. 1983 Independent Research and Development Technical Plan, General Electric Company, Aircraft Engine Business Group, R83AEB263, Vol. V, 1983.

32. Siemers, P.A. and Hillig, W.B., "Thermal Barrier Coated Turbine Blade Study", NASA CR-165351, 1981.

33. Palko, J.E., Luthra, K.L., and McKee, D.W., "Evaluation of Performance of Thermal Barrier Coatings Under Simulated Industrial/Utility Gas Turbine Conditions", Final Report D.O.E., Contract NO. EC-77-C-05-5402, 1978.

34. Zaplatynsky, I., "Reactions of Yttria-Stabilized Zirconia With Oxides and Sulfates of Various Elements", NASA TM-78942, 1978.

1. Report No.	2. Government Accession No.	3. Recipient's Catalog No.
NASA CR - 175010		

4. Title and Subtitle	5. Report Date
Thermal Barrier Coating Life Prediction Model	April, 1985
	6. Performing Organization Code

7. Author(s)	8. Performing Organization Report No.
R. V. Hillery, B. H. Pilsner	R85AEB304
	10. Work Unit No.

9. Performing Organization Name and Address	11. Contract or Grant No.
General Electric Company Evendale, Ohio 45215-6301	

12. Sponsoring Agency Name and Address	13. Type of Report and Period Covered
National Aeronautics and Space Administration Washington, D.C. 20546	First Annual Contractor Report
	14. Sponsoring Agency Code

15. Supplementary Notes

Project Manager, James A. Nesbitt, Materials Division,
NASA Lewis Research Center, Cleveland, Ohio

16. Abstract

This is the first annual report of the first phase of a 3-year program. The objectives of the program are to determine the predominant modes of degradation of a plasma sprayed thermal barrier coating system, and then to develop and verify life prediction models accounting for these degradation modes. The first task (Task I) is to determine the major failure mechanisms. Presently, bond coat oxidation and bond coat creep are being evaluated as potential TBC failure mechanisms. The baseline TBC system consists of an air plasma sprayed ZrO_2-Y_2O_3 top coat, a low pressure plasma sprayed NiCrAlY bond coat, and a Rene'80 substrate. Pre-exposures in air and argon combined with thermal cycle tests in air and argon are being utilized to evaluate bond coat oxidation as a failure mechanism. The first experiment has been completed. Unexpectedly, the specimens pre-exposed in argon failed before the specimens pre-exposed in air in subsequent thermal cycles testing in air.

Four bond coats with different creep strengths are being utilized to evaluate the effect of bond coat creep on TBC degradation. These bond coats received an aluminide overcoat prior to application of the top coat to reduce the differences in bond coat oxidation behavior. Thermal cycle testing of these specimens has been initiated.

Methods have been selected for measuring tensile strength, Poisson's ratio, dynamic modulus and coefficient of thermal expansion both of the bond coat and top coat layers.

17. Key Words (Suggested by Author(s))	18. Distribution Statement
Thermal Barrier Coatings Life Prediction Methodology Failure Mechanisms Coating Properties	Unclassified - Unlimited

19. Security Classif. (of this report)	20. Security Classif. (of this page)	21. No. of Pages	22. Price*
Unclassified	Unclassified	66	

* For sale by the National Technical Information Service, Springfield, Virginia 22161